Stationary waves on nonlinear quantum graphs I:
General framework and canonical perturbation theory

Sven Gnutzmann

School of Mathematical Sciences, University of Nottingham, Nottingham NG7 2RD, UK

Daniel Waltner

Fakultät für Physik, Universität Duisburg-Essen, Lotharstraße 1, 47048 Duisburg, Germany

In this paper we present a general framework for solving the stationary nonlinear Schrödinger equation (NLSE) on a network of one-dimensional wires modelled by a metric graph with suitable matching conditions at the vertices. A formal solution is given that expresses the wave function and its derivative at one end of an edge (wire) nonlinearly in terms of the values at the other end. For the cubic NLSE this nonlinear transfer operation can be expressed explicitly in terms of Jacobi elliptic functions. Its application reduces the problem of solving the corresponding set of coupled ordinary nonlinear differential equations to a finite set of nonlinear algebraic equations. For sufficiently small amplitudes we use canonical perturbation theory which makes it possible to extract the leading nonlinear corrections over large distances.

I.   INTRODUCTION

In a series of two papers we treat stationary solutions on nonlinear quantum graphs and introduce an approach based on canonical perturbation theory. This is the first paper in the series where we deal with the general theoretical framework. In the second paper [1] we will apply the framework to a set of basic graph structures.

Linear quantum graphs where the wave function obeys the linear Schrödinger equation on the edges with suitable matching conditions have attracted a lot of attention in physics and mathematics in the past (see [2–4] and references therein). In quantum chaos they serve as a paradigm model that makes it possible to analyze spectral fluctuations [2, 3, 5, 6], wave function statistics [7] and chaotic scattering [8–10]. More generally they are paradigm models for the effects of nontrivial topologies on wave function propagation. Nonlinear quantum graphs replace the linear wave equations with a nonlinear wave equation and have the potential of becoming a paradigm model for topological effects in nonlinear wave propagation because they are sufficiently simple to allow for comparatively straight forward numerical analysis and analytical approaches while showing fundamentally nonlinear effects (such as multistability or bifurcations).

Physically they can be considered as models for wave propagation in optical networks and quasi-one-dimensional (cigar-like) Bose-Einstein condensates [11]. In either optical systems or Bose-Einstein condensates nonlinear effects enter naturally. In the optical systems this is due to nonlinear media (Kerr effect) and in Bose-Einstein condensates it is due to the boson-boson interaction. It is then required to add nonlinear terms to the Schrödinger equation, which makes explicit analysis generally much harder. One is often restricted to either numerical analysis (see, e.g., [12]), diagrammatic approaches valid for small nonlinearities (see, e.g., [13]) or to one spatial dimension [14, 15].

Adding nonlinear terms to the wave equation on a quantum graph results in a nonlinear quantum graph. A numerical survey [16] showed the importance of nonlinear effects in stationary scattering from a nonlinear graph even if the incoming waves have very low intensity. As has been revealed later [17], this is partly due to the presence of very narrow (so-called topological) resonances. Stationary solutions on nonlinear quantum graphs have been discussed for some basic graph structures [18]. For a general nonlinearity proportional to $|\psi|^{2\nu}\psi$, stationary states on a star graph were considered [19–21]. The phase space structure was analyzed on a three edge star graph [22] and the stability of the states was studied [23]. On a tadpole graph bifurcations and stability of stationary solutions have been analyzed [24, 25].

Some time-dependent solutions have been considered. The propagation of a soliton through a vertex in a star graph was analyzed in [26–30]. Interacting Bose liquids in Y-junctions and ring geometries [31] and H-shaped potentials [32] or several differently connected branches of discrete nonlinear networks [33–35] may also be considered as nonlinear quantum graphs. An experimental realization of one-dimensional scattering in optical nonlinear media is reported in [36]; the escape of solitons in [37]. A recent review by Noja [38] summarizes nicely some of the more mathematical approaches mentioned above.

Our first aim in this paper is to reduce the coupled nonlinear differential equations to a finite set of nonlinear algebraic equations. Such a reduction requires the solution of the nonlinear transfer problem; i.e., one needs to express the wave function and its derivative at one end of an edge in terms of the values at the other end. We give

a general formal solution to this problem. For the cubic nonlinearity these can be expressed explicitly using Jacobi elliptic functions. In an extensive appendix we give the complete set of solutions in this case. This extends the known explicit stationary wave functions on a line or a circle [39, 40]. The second aim is to develop a perturbation theory that simplifies the formal transfer solution such that analytical methods can be used to find approximate wave functions on a graph.

In Section II we give the general framework and discuss general properties of the stationary solutions: We define nonlinear quantum graphs, describe how to obtain local solutions on the edges and explain how to reduce the general problem of finding stationary solutions to a finite set of nonlinear algebraic equations. In Section III we introduce a perturbative treatment of the nonlinearity in the framework of canonical perturbation theory. Two extensive Appendixes A and B contain detailed explicit solutions for the cubic NLSE for reference.

II.   NONLINEAR QUANTUM GRAPHS

A.   General Setting

We consider a general graph $\mathcal{G}(\mathcal{V}, \mathcal{E})$ where $\mathcal{V}$ is a set of vertices and $\mathcal{E}$ a set of edges. In standard graph theory each edge $e \in \mathcal{E}$ connects two vertices $v_1, v_2 \in \mathcal{V}$. If $v_1 = v_2$, the edge is called a loop. Two different vertices $v_1 \neq v_2$ are called adjacent or connected if there is an edge that connects them. In this case we also say that the edge is connected or adjacent to the vertices v_1 and v_2. In the present context it is useful to generalize the notion of a graph slightly and allow for *semi-infinite* edges that are only connected to one vertex (formally one may think of this as a standard graph with one vertex 'at infinity' that collects all the loose ends). We call the semi-infinite edges *leads* and all edges that connect two vertices (including loops) *bonds*. The corresponding sets of leads and bonds are denoted by $\mathcal{L}$ and $\mathcal{B}$ and we have $\mathcal{E} = \mathcal{L} \cup \mathcal{B}$ and $\mathcal{L} \cap \mathcal{B} = \varnothing$. We only consider *finite* graphs where the number of vertices $V = |\mathcal{V}|$ and edges $E = |\mathcal{E}|$ are both finite. The numbers of leads $L = |\mathcal{L}|$ of and bonds $B = |\mathcal{B}|$ are then also finite and $E = B + L$. If a graph has no leads $L = 0$ we call it a *closed graph*, if it has at least one lead $L \geq 1$ then we call it an *open graph*. Figure 1 shows examples of open and a closed graphs.
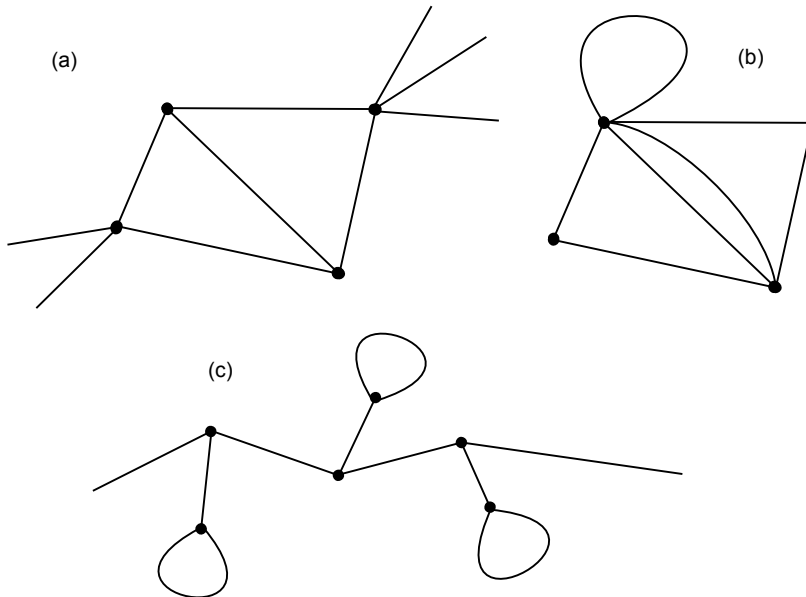

FIG. 1. Examples of network structures: a finite open graph (a); a finite closed graphs (b). If the structure of the graph (c) is continued one obtains an infinite graph.

In a quantum graph each edge models a waveguide or string with waves propagating along them. This is realized by adding a metric and a well-defined wave equation on the graph. In a metric graph each edge has a length $\ell_e > 0$, and a coordinate $x_e \in [0, \ell_e]$. For any bond $b \in \mathcal{B}$ the length is finite $\ell_b < \infty$ and $x_b = 0$ and $x_b = \ell_b$ correspond to the endpoints of the edge. For each lead $l \in \mathcal{L}$ the length is infinite $\ell_l = \infty$, and $x_\ell = 0$ at the vertex attached to the lead. This structure defines the distance between two points anywhere on the graph in an obvious way as the length of the shortest connected path through the graph that connects the two points [41].

We consider a scalar complex wave function on the metric graph which is differentiable with respect to t and with respect to x on the edges. It is written as a collection,

$$\Psi(x;t) = \{\psi_e(x_e;t)\}_{e\in\mathcal{E}}, \tag{1}$$

where $\psi_e(x_e;t)$ is the wave functions on the edge e at time t. The wave function on edge e satisfies the nonlinear Schrödinger equation (NLSE)

$$i\partial_t\psi_e = -\partial_{x_e}^2\psi_e + g_e|\psi_e|^{2\nu}\psi_e \ . \tag{2}$$

Here, $\nu > 0$ characterizes the power of the nonlinearity and g_e is the real nonlinear coupling parameter which we assume constant and finite $|g_e| < \infty$ on each edge. The nonlinear coupling term is called repulsive for $g_e > 0$ and attractive for $g_e < 0$. Without loss of generality we use units where Planck's constant and the mass take values $\hbar = 2m = 1$ everywhere in this paper. The *cubic* NLSE that is relevant for Bose-Einstein condensates or optical media is obtained when $\nu = 1$ – in this case the nonlinear term $g|\psi|^2\psi$ is cubic in ψ. The quintic case $\nu = 2$ with nonlinear term $g|\psi|^4\psi$ also finds some applications [42].

Matching conditions at the vertices need to be added to have a well-posed propagation of an initial wave function $\Psi_0(x)$. For linear quantum graphs the most general matching conditions that result in a self-adjoint problem have been given in [43] (see also [4]). All of these remain mathematically and physically sound in the nonlinear setting (and may be generalized by allowing nonlinear matching conditions). Here we focus on the so-called δ-type (or Robin) conditions. For a given vertex v let us assume (without loss of generality) that $x_e = 0$ corresponds to the endpoint at v for all edges e adjacent to v. Then δ-type matching conditions at v are defined by two conditions:

i. The wave function is continuous through the vertex,

$$\psi_e(0;t) = \psi_{e'}(0;t) \equiv \psi_0, \tag{3}$$

for all pairs of edges $e, e' \in \mathcal{E}(v)$ and all times t. By definition, $\mathcal{E}(v)$ is the set of all edges connected to the vertex v.

ii. The sum of outward derivatives of the wave function on the adjacent edges is proportional to the value of the wave function on the vertex

$$\sum_{e\in\mathcal{E}(v)} \partial_{x_e}\psi_e(0;t) = \lambda\psi_0 \ . \tag{4}$$

Here λ is a real parameter, the *vertex potential*. For a vertex of valency two this condition is equivalent to a δ-potential of strength λ on an interval (the position of the δ-potential marking the position of the vertex). For $\lambda < 0$ we call the vertex attractive and for $\lambda > 0$ repulsive. In most applications that we discuss later we choose $\lambda = 0$. Then the matching conditions are also known as standard (aka free, Kirchhoff or Neumann) matching conditions [44].

In the linear setting ($g = 0$) these conditions lead to a self-adjoined extension of the metric Laplacian on the graph (i.e., a well-defined Schrödinger operator). The first condition is physically reasonable and the second ensures that the L^2 norm of the wave function

$$\|\Psi(x;t)\|^2 = \sum_{e\in E} \int_0^{\ell_e} |\psi_e(x_e;t)|^2 dx_e \tag{5}$$

is conserved. Physically, the L^2 norm corresponds to the number of particles (number of atoms in a Bose-Einstein condensate, number of photons or total intensity in optics). If $g_e = 0$ for all edges e, Eq. (2) becomes the (free) Schrödinger equation on a metric graph and the model becomes a quantum graph. For quantum graphs wave propagation is described by linear differential equations. If $g_e \neq 0$ on some edge the differential equations are non-linear and we call the model *nonlinear quantum graph*. Note that a nonlinear quantum graph can be used as a model of either a quantum mechanical system (Bose-Einstein condensate) or a purely classical wave system (electromagnetic waves in optical fibres).

Generally, one is interested in the time-dependent dynamics of an (square integrable and sufficiently smooth) initial wave function $\Psi_0(x) = \{\psi_{e,0}(x_e)\}_{e\in\mathcal{E}}$. For an infinite line this problem is formally solved by the so-called inverse scattering method [45], which is practical only for soliton-like solutions. For a half line or an interval with appropriate boundary conditions (e.g. Dirichlet) the problem of finding any time-dependent solutions is highly nontrivial. The

generalization of the method to star graphs has recently been discussed in [30]. In this paper we focus on stationary solutions of the form

$$\Psi(x;t) = e^{-i\mu t}\Phi(x) \quad \Rightarrow \quad \psi_e(x_e;t) = e^{-i\mu t}\phi_e(x_e) \ . \tag{6}$$

The function $\Phi(x) = \{\phi_e(x_e)\}_{e=1}^{E}$ is then a collection of solutions of the stationary NLSE

$$-\frac{d^2\phi_e}{dx_e^2} + g_e|\phi_e|^{2\nu}\phi_e = \mu\phi_e \tag{7}$$

on each edge with the matching conditions (3) and (4) applied to $\Phi(x)$. We refer to the parameter μ as the chemical potential (in accordance with the physics literature on Bose-Einstein condensation).

B. Formal Local Solutions on a Given Edge

Before discussing stationary solutions for a complete graph let us first consider a single fixed edge e. We will suppress the index e until we come back to the discussion of the full graph. The length of the edge is ℓ and we assume that the wave function and its derivative are given at $x = 0$. Our aim is to find the nonlinear transfer operator that expresses the wave function and its derivative at $x = \ell$ in terms of their values at $x = 0$. We will show that this is formally equivalent to the solution of an initial value problem for a central force dynamics of a two-dimensional mass point in the plane with a central potential where x takes the formal role of a time. The latter being integrable, it is straight-forward to write a formal solution using textbook methods of analytical mechanics. Let us here summarize this approach and set

$$\phi(x) = r(x)e^{i\eta(x)} \tag{8}$$

with real amplitude $r(x) \geq 0$ and real phase $\eta(x)$. The NLSE is then expressed as two coupled real ordinary differential equations,

$$\frac{d^2r}{dx^2} = r\frac{d\eta}{dx}^2 + gr^{2\nu+1} - \mu r \quad \text{and} \quad \frac{d}{dx}\left[\frac{d\eta}{dx}r^2\right] = 0 \ . \tag{9}$$

If x is formally considered a time these equations are the Euler-Lagrange equations for a point particle in the plane in polar coordinates with a central potential

$$V(r) = \frac{\mu}{2}r^2 - \frac{g}{2\nu+2}r^{2\nu+2} \ . \tag{10}$$

The angular momentum

$$p_\eta = r^2\frac{d\eta}{dx} = \text{Im}\,\phi^*\frac{d\phi}{dx} \tag{11}$$

and the Hamiltonian energy

$$H = \frac{1}{2}\frac{dr}{dx}^2 + \frac{p_\eta^2}{2r^2} + V(r) \tag{12}$$

are the two well-known constants of motion. Note that in terms of the original NLSE p_η is the intensity (or probability) flow. As is well known, the radial motion then reduces effectively to a mass point in the effective potential

$$V_{\text{eff}}(p_\eta, r) = \frac{p_\eta^2}{2r^2} + V(r). \tag{13}$$

Let us denote the solutions of the dynamical system with initial values

$$\phi(0) = r_0 e^{i\eta_0} \quad \text{and} \quad \frac{d\phi}{dx}(0) = \left(\sigma\sqrt{2(H - V_{\text{eff}}(r_0))} + i\frac{p_\eta}{r_0}\right)e^{i\eta_0} \tag{14}$$

(with $\sigma = \pm 1$) as

$$r(x) = R_{g,\mu}(x; r_0, p_\eta, H, \sigma) \quad \text{and} \quad \eta(x) = \eta_0 + \vartheta_{g,\mu}(x; r_0, p_\eta, H, \sigma) \tag{15}$$

where the two functions $R_{g,\mu}(x; r_0, p_\eta, H, \sigma) > 0$ and $\vartheta_{g,\mu}(x; r_0, p_\eta, H, \sigma)$ are implicitly defined through the two integrals

$$x = \sigma \int_{r_0}^{R_{g,\mu}(x; r_0, p_\eta, H, \sigma)} \left(2(H - V_{\text{eff}}(p_\eta, r))\right)^{-1/2} dr \tag{16a}$$

$$\vartheta_{g,\mu}(x; r_0, p_\eta, H, \sigma) = p_\eta \int_0^x R_{g,\mu}(x'; r_0, p_\eta, H, \sigma)^{-2} dx' . \tag{16b}$$

We often just write $R_{g,\mu}(x)$ and $\vartheta_{g,\mu}(x)$ if the values of the other parameters are clear from context. On the level of the NLSE these two functions implicitly define the nonlinear transfer operator by evaluating them and their derivatives at $x = \ell$. Note that the integral (16a) defines $R_{g,\mu}(x; r_0, p_\eta, H, \sigma)$ if x is sufficiently small; for bounded solutions this can be extended to arbitrary large values of x. The sign $\sigma = \pm 1$ is positive (negative) if $R_{g,\mu}(x; r_0, p_\eta, H, \sigma)$ is increasing (decreasing) as a function of x at $x = 0$.

If the nonlinear coupling constant vanishes ($g = 0$) the explicit expressions for $R_{0,\mu}(x)$ and $\vartheta_{0,\mu}(x)$ can be obtained from the known (local) solutions of the linear Schrödinger equation

$$R_{0,\mu}(x)e^{i\vartheta_{0,\mu}(x)} = \begin{cases} r_0 \cos(kx) + \frac{\sigma\sqrt{2Hr_0^2 - p_\eta^2 - k^2 r_0^4} + ip_\eta}{kr_0} \sin(kx) & \text{if } \mu = k^2 > 0 \\ r_0 + \frac{\sigma\sqrt{2Hr_0^2 - p_\eta^2} + ip_\eta}{r_0} x & \text{if } \mu = 0 \\ r_0 \cosh(kx) + \frac{\sigma\sqrt{2Hr_0^2 - p_\eta^2 + k^2 r_0^4} + ip_\eta}{kr_0} \sinh(kx) & \text{if } \mu = -k^2 < 0. \end{cases} \tag{17}$$

The problem of finding solutions for arbitrary values of the chemical potential $\mu \neq 0$ and nonlinear coupling constants $g \neq 0$ can be reduced to a few standard solutions due to the scaling laws

$$R_{g,\mu}(x; r_0, p_\eta, H, \sigma) = R_{\frac{g}{k^2}, \pm 1}\left(kx; r_0, \frac{p_\eta}{k}, \frac{H}{k^2}, \sigma\right) \tag{18a}$$

$$\vartheta_{g,\mu}(x; r_0, p_\eta, H, \sigma) = \vartheta_{\frac{g}{k^2}, \pm 1}\left(kx; r_0, \frac{p_\eta}{k}, \frac{H}{k^2}, \sigma\right) \tag{18b}$$

where $k = \sqrt{|\mu|} > 0$ and

$$R_{g,\mu}(x; r_0, p_\eta, H, \sigma) = \alpha R_{\pm 1, \mu}\left(x; \frac{r_0}{\alpha}, \frac{p_\eta}{\alpha^2}, \frac{H}{\alpha^2}, \sigma\right) \tag{19a}$$

$$\vartheta_{g,\mu}(x; r_0, p_\eta, H, \sigma) = \vartheta_{\pm 1, \mu}\left(x; \frac{r_0}{\alpha}, \frac{p_\eta}{\alpha^2}, \frac{H}{\alpha^2}, \sigma\right) \tag{19b}$$

where $\alpha = |g|^{-\frac{1}{2\nu}}$.

For a given exponent $\nu > 0$ it suffices to consider the cases $g = \pm 1$ and $\mu = \pm 1$ in order to get all local solutions for arbitrary values g and μ – the case $\mu = 0$ is included by taking the limits

$$R_{g,0}(x; r_0, p_\eta, H, \sigma) = \lim_{k \to 0} R_{g,1}(kx; r_0, p_\eta/k, H/k^2, \sigma) \tag{20a}$$

$$\vartheta_{g,0}(x; r_0, p_\eta, H, \sigma) = \lim_{k \to 0} \vartheta_{g,1}(kx; r_0, p_\eta/k, H/k^2, \sigma) \tag{20b}$$

and the limit $g \to 0$ needs to be consistent with (17).

For the cubic NLSE the functions $R_{\pm 1, \pm 1}(x; r_0, p_\eta, H, \sigma)$ and $\vartheta_{\pm 1, \pm 1}(x; r_0, p_\eta, H, \sigma)$ can be expressed explicitly in terms of Jacobi elliptic functions (see Appendix A). For general ν we could not express the integrals (16a) and (16b) in terms of any known special functions. The qualitative behavior of these solutions follows straight forwardly from the form of the effective potential $V_{\text{eff}}(r)$. While this is all well known, it is useful in the present context to summarize the various cases. We do this in the rest of this section, adding some remarks related to their use in nonlinear quantum graphs.

1. The repulsive case $g > 0$

It is sufficient to consider $g = 1$ and $\mu = \pm 1$. The solutions $R_{1, \pm 1}(x; r_0, p_\eta, H, \sigma)$ and $\vartheta_{1, \pm 1}(x; r_0, p_\eta, H, \sigma)$ depend mainly on the two parameters H and p_η – i.e. the Hamiltonian energy and the angular momentum in the auxiliary
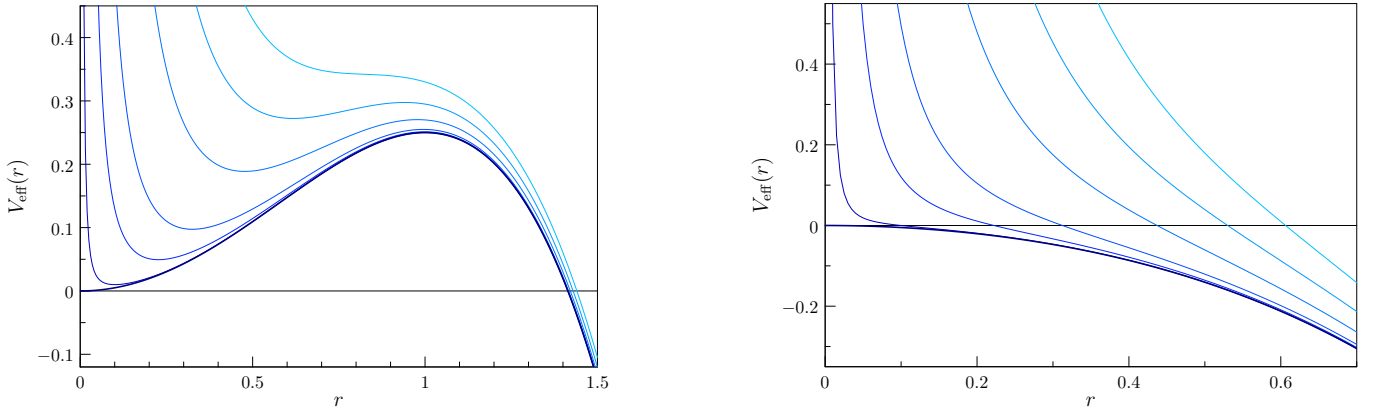
FIG. 2. (Color Online) The effective potential $V_{\text{eff}}(r)$ for the radial motion in the auxiliary dynamical system with repulsive non-linear coupling $g = 1$ and $\nu = 1$. In the left graph the chemical potential is $\mu = 1$; in the right graph $\mu = -1$. The curves in each graph correspond to different values of the flow (angular momentum of auxiliary dynamics) $p_\eta = (0, 0.01, 0.05, 0.1, 0.2, 0.3, 0.4)$. Graphs for different values of the exponent ν look qualitatively similar.
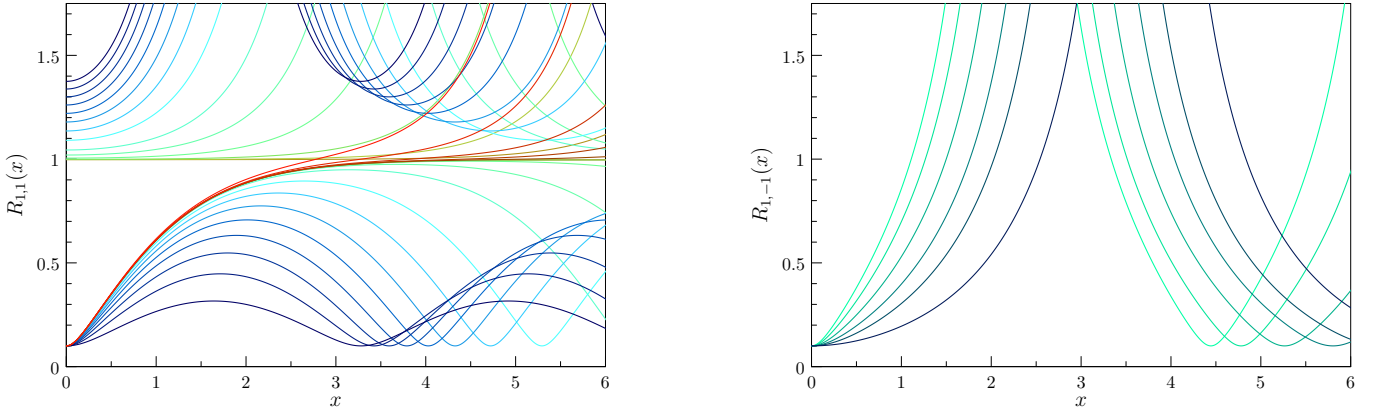

FIG. 3. (Color Online) The amplitude functions $R_{1,1}(x)$ (left) and $R_{1,-1}(x)$ (right) for local solutions of the NLSE with repulsive interaction. The parameters H, p_η have been varied and r_0 such that minimal amplitude is obtained for $x = 0$. For $R_{1,1}(x)$ bounded and unbounded solutions are shown. The plotted functions are for $\nu = 1$ ($\nu \neq 1$ leads to qualitatively similar solutions).

central potential dynamics in the plane. The dependence on r_0 and σ is just a matter of shifting the origin $x \mapsto x - x_0$, i.e., translating a solution. For the qualitative discussion we consider the effective potential

$$V_{\text{eff}}(r) = \frac{p_\eta^2}{2r^2} \pm \frac{r^2}{2} - \frac{1}{2\nu + 2} r^{2\nu+2} \qquad (21)$$

of the radial motion, where the sign is chosen positive (negative) for $\mu = 1$ ($\mu = -1$). Figure 2 shows the effective potential for various values of the angular momentum p_η. For positive chemical potential $\mu > 0$ we see the following different types of solutions.

i. For $|p_\eta| < p_{\text{crit}} \equiv \left(\frac{\nu}{\nu+2}\right)^{1/2} \left(\frac{2}{\nu+2}\right)^{1/\nu}$ the effective potential has a local minimum and a local maximum at energies $H = \mathcal{E}_{\text{min}}(p_\eta)$ and $H = \mathcal{E}_{\text{max}}(p_\eta)$ (see Figure 2). For energies between these two energies $\mathcal{E}_{\text{min}} \leq H \leq \mathcal{E}_{\text{max}}$, there is a bounded solution where $r_1 \leq R_{1,1}(x) \leq r_2$ and an unbounded solution $R_{1,1}(x) > r_3$ (see Figure 2).

For the bounded solutions the amplitude is a periodic function $R_{1,1}(x) = R_{1,1}(x + \Lambda_{1,1})$ with period

$$\Lambda_{1,1}(H, p_\eta) = 2 \int_{r_1}^{r_2} \left(2H - \frac{p_\eta^2}{r^2} - r^2 + \frac{1}{\nu+1} r^{2\nu+2} \right)^{-1/2} dr \; . \qquad (22)$$

This period tends to infinity when $H \to \mathcal{E}_{\max}(p_\eta)$ from below. In that case the amplitude $R_{1,1}(x)$ tends to the constant value $r_{\max}(p_\eta)$ for $x \to \pm\infty$ and has a single minimum at a finite x value. Because of the corresponding dip in the amplitude such solutions are known as dark stationary solitons [46] though this name is sometimes reserved to the case $p_\eta = 0$ where the intensity vanishes at one point. Figure 3 shows plots for the amplitude $R_{1,1}(x)^2$ for various parameters including dark solitons.

The phase function $\vartheta_{1,1}(x)$ is an increasing (decreasing) function if $p_\eta > 0$ ($p_\eta < 0$). In general, $\Delta\vartheta = \vartheta_{1,1}(x+\Lambda_{1,1}) - \vartheta_{1,1}(x)$ is not a rational multiple of π, so the corresponding wave functions $\phi(x) = R_{1,1}(x)e^{i\vartheta_{1,1}(x)}$ are, in general, not periodic functions of x. The wave function $\phi(x) = R_{1,1}(x)e^{i\vartheta_{1,1}(x)}$ is real if and only if $p_\eta = 0$. The phase does not change as long as the amplitude is positive. When $R_{1,1}(x) = 0$ the wave function has a nodal point and changes its sign; i.e., $\vartheta_{1,1}(x)$ changes by π. Indeed, it is clear from the form of $V_{\mathrm{eff}}(r)$ that $p_\eta = 0$ if $\phi(x)$ has nodal points. It can be shown explicitly that expression (16b) for the phase shows a discontinuous jump by $\pm\pi$ in the limit $p_\eta \to 0$.

ii. For $|p_\eta < p_{\mathrm{crit}}|$ and either $H > \mathcal{E}_{\max}$ or $H < \mathcal{E}_{\min}$ all solutions are unbounded.

iii. For $|p_\eta > p_{\mathrm{crit}}|$ the local extrema of the effective potential have disappeared and it becomes a strictly decreasing function. In this case only unbounded solutions exist.

For negative chemical potential $\mu < 0$ the effective potential is a decreasing function and only unbounded solutions exist.

The bounded solutions for positive chemical potential can be extended to global solutions on the infinite line straight forwardly. All unbounded solutions develop a singularity at a finite value x_{sing}, where amplitude $R_{1,\pm1}(x; r_0, p_\eta, H, \sigma)$ diverges like $1/|x - x_{\mathrm{sing}}|^{1/\nu}$ as can be checked by inserting a wave function with that kind of singularity in the stationary NLSE. Physically, such singularities indicate a breakdown of the model as the NLSE is usually an effective description of a physical system that is valid only for sufficiently small amplitudes. Moreover, for $0 < \nu \leq 2$ the corresponding wave functions are not square integrable over a finite interval containing the singularity ($\int_{x_{\mathrm{sing}}}^{x_{\mathrm{sing}}+\Delta x} |\Phi(x)|^2 dx \sim \int_0^{\Delta x} x^{-2/\nu} dx$ diverges). For a Bose-Einstein condensate ($\nu = 1$) this implies infinitely many particles in a small interval around the singularity which is also not physical. One is tempted to focus just on the globally bounded solutions. However, in the present setting we want to use local solutions on finite intervals to construct solutions on a graph; in that setting the globally unbounded solutions cannot be excluded as they may still describe bounded solutions on an edge of finite length (the singularity may only develop on a larger distance). It is not difficult to construct global bounded solutions on a chain or ring graph which involve any of the local solutions discussed above.
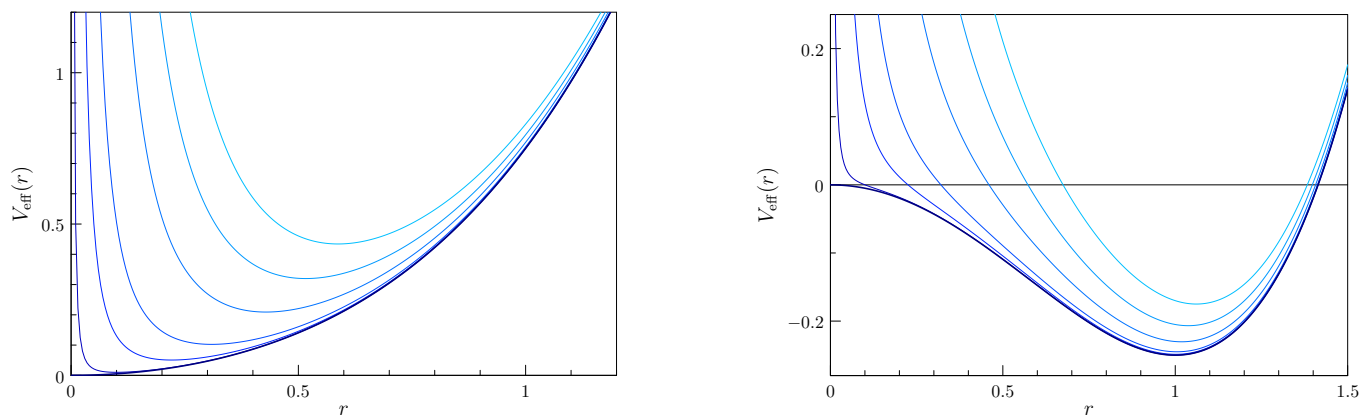
2. The attractive case $g < 0$

FIG. 4. (Color Online) The effective potential $V_{\mathrm{eff}}(r)$ for the radial motion in the auxiliary dynamical system with attractive nonlinear coupling $g = -1$ and $\nu = 1$. In the left graph the chemical potential is $\mu = 1$; in the right graph it is $\mu = -1$. The curves in each graph correspond to different values of the flow (angular momentum of auxiliary dynamics) $p_\eta = (0, 0.01, 0.05, 0.1, 0.2, 0.3, 0.4)$.

Graphs for different values of the exponent ν look qualitatively similar.
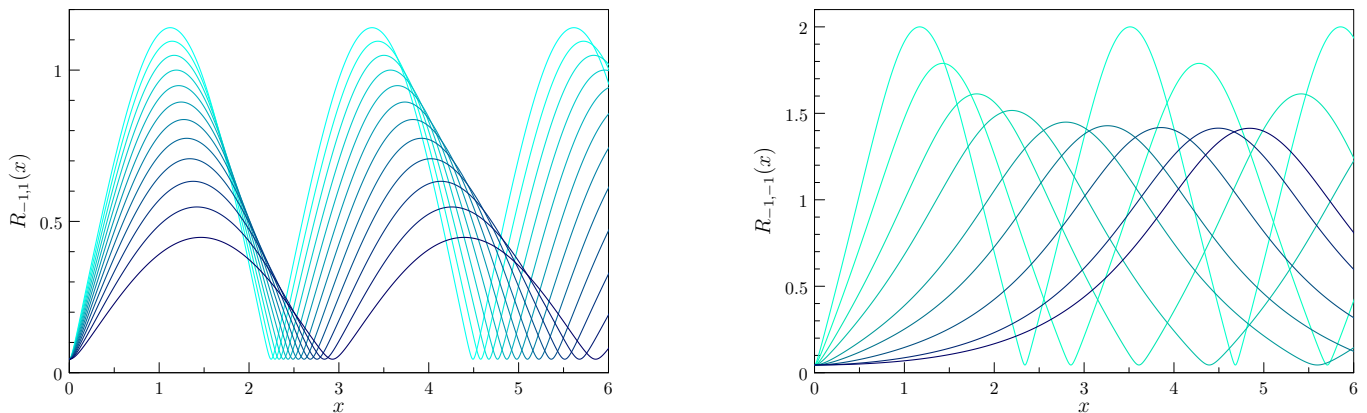
FIG. 5. (Color Online) The amplitude functions $R_{-1,1}(x)$ (left) and $R_{-1,-1}(x)$ (right) for local solutions of the NLSE with repulsive interaction. The parameters H, p_η have been varied and r_0 chosen such that the minimum is at $x = 0$. The plotted functions are for $\nu = 1$ ($\nu \neq 1$ leads to qualitatively similar solutions).

Here it is sufficient to consider $g = -1$ and $\mu = \pm 1$. The effective potential is

$$V_{\text{eff}} = \frac{p_\eta^2}{2r^2} \pm \frac{r^2}{2} + \frac{1}{2\nu + 2}r^{2\nu+2}. \tag{23}$$

Figure 4 shows the effective potential for various values of p_η. Stationary solutions in the attractive case always remain bounded with an amplitude $r_1 \leq R_{-1,\pm1}(x) \leq r_2$ (where the values of the turning points r_1 and r_2, depend on p_η, H and the sign of $\mu = \pm 1$). The amplitude is a periodic function $R_{-1,\pm1}(x) = R_{-1,\pm1}(x + \Lambda_{-1,\pm1})$ with period

$$\Lambda_{-1,\pm1}(H, p_\eta) = 2\int_{r_1}^{r_2} \left(2H - \frac{p_\eta^2}{r^2} \mp r^2 - \frac{1}{\nu+1}r^{2\nu+2}\right)^{-1/2} dr . \tag{24}$$

This period is finite unless $p_\eta = 0$ and $H = 0$ for a negative chemical potential $\mu < 0$. The solution in this case consists of a single peak at $x = 0$ which falls off exponentially on both sides and then drops monotonically to zero as $|x| \to \infty$. This solution is known as a stationary soliton [46]. Figure 5 shows plots for the amplitude $R_{-1,\pm1}(x)$ for various parameters including the soliton.

The phase function $\vartheta_{-1,\pm1}(x)$ is again an increasing (decreasing) function if $p_\eta > 0$ ($p_\eta < 0$) such that $\Delta\vartheta = \vartheta_{-1,\pm1}(x + \Lambda_{-1,\pm1}) - \vartheta_{-1,\pm1}(x)$ is in general not a rational multiple of π. In the attractive case the wave function $\phi(x) = R_{-1,\pm1}(x)e^{i\vartheta_{-1,\pm1}(x)}$ is real if and only if there are nodal points on the infinite line (which is equivalent to $p_\eta = 0$).

C. Stationary States for a Closed Graph as a Nonlinear Eigenproblem

Let us now assume that we have a finite (connected) closed graph with $E = B < \infty$ edges all of which are bonds. For the *linear* Schrödinger equation on such a graph (i.e. if the nonlinear coupling constants vanish on each edge, $g_e = 0$ for all $e \in \mathcal{E}$) it is well known that stationary solutions only exist for a discrete set of values μ_n of the chemical potential. In the context of the linear Schrödinger operator these are the energy eigenvalues of the system and the collection $\{\mu_n\}_{n=0}^\infty$ is the linear spectrum of the graph. Spectral theory for linear quantum graphs is well developed [2–4]. Before developing the approach to nonlinear quantum graphs, let us summarize how the linear spectrum is characterized as the zero of an explicit characteristic function $\xi(k)$. Denoting a directed bond as a pair (b, d), where b denotes the bond and $d = \pm 1$ is the direction such that $d = 1$ ($d = -1$) is the direction in which x_b increases (decreases). For positive chemical potential $\mu = k^2 > 0$ the characteristic function has the form

$$\xi(k) = \det(1 - e^{ik\ell}S) \tag{25}$$

where S is a unitary $2B \times 2B$ matrix that contains the quantum amplitudes to scatter from one directed edge (b, d) into another directed edge (b', d') and $e^{ik\ell} = \text{diag}\left(e^{ik\ell_1}, \ldots, e^{ik\ell_B}, e^{ik\ell_1}, \ldots, e^{ik\ell_B}\right)$ is a $2B \times 2B$ diagonal (unitary) matrix that contains the phases $e^{ik\ell_b}$ that a plane wave acquires going from one end of an edge to the other. The matrix S

contains information about the connectivity and about the matching conditions. Its matrix elements $S_{bd,b'd'}$ vanish unless the terminal vertex of the directed edge (b', d') is the same as the starting vertex of (b, d). The nonvanishing values $S_{bd,b'd'}$ depend on the matching conditions. Eq. (25) (or some relative of it) can be used as the starting point for developing many tools of spectral theory, such as trace formulas which express spectral functions (e.g. the number of states inside a spectral interval) in terms of periodic walks on the graph [2]. In the linear case one may always normalize a solution such that $\|\Phi_n(x)\|^2 = 1$.

Let us now come back to the nonlinear case where stationary solutions can, in general, not be multiplied by scalars and remain stationary solutions. Spectrum and eigenfunctions of the linear quantum graph remain relevant for a nonlinear quantum graph when the L^2-norm

$$N = \|\Phi(x)\|^2 \tag{26}$$

is small, i.e., when we take $N \to 0$ we expect to recover the linear spectrum and the linear eigenfunctions (up to normalization). For arbitrary values of N we see that stationary solutions exist along one-parameter families of values for the chemical potential $\mu_n(N)$.

This can be seen by constructing global solutions on the graph from local solutions and adding matching conditions on the graph. If one first disregards any matching conditions, one may take the values of the wave function $\phi_e(x_e)$ and its derivative at the point $x_e = 0$ as free parameters. The local solutions of the NLSE imply the local transfer operator that allows us to find the corresponding values at the other end of the edge $x_e = \ell_e$. This gives $4B$ independent real parameters to which we now add the matching conditions. Continuity at one vertex i of valency v_i implies $2(v_i - 1)$ real conditions; adding over all vertices, this implies $4B - 2V$ independent real conditions. Next we have the condition (4) for each vertex. These give together $2V - 1$ independent real conditions. Note that one may have expected $2V$ conditions; however, the imaginary part of the matching condition (4) refers to flux conservation which is also conserved by the solutions along the edge. So if the flux condition is met at $V - 1$ vertices it will automatically be conserved at the last vertex as well. On the other side we are free to choose an overall phase which adds one more condition. Note that flux conservation is related to this global gauge symmetry by Noether's theorem, so in a sense the 'missing' condition we observed for flux conservation at each vertex reappears in the form of one parameter that we are free to choose. Altogether we have as many conditions as free variables. So for given μ there will generically be solutions for isolated points in the parameter space that solve the problem. Each of these will have a definite value for the norm N. If we fix N from outside we have to leave μ as a free parameter and will generically obtain solutions for discrete values $\{\mu_n(N)\}$ of the chemical potential. As N is changed the chemical potential of a given solution will change and the corresponding wave function will deform. In principle, bifurcations may occur when N is changed; i.e., solutions may coalesce and disappear, or solutions may appear. In order to define a generalized eigenvalue problem, one may fix N; in that case the nonlinear spectrum $\{\mu_n(N)\}_{n=0}^{\infty}$ will generally remain a discrete set. Note that it is, in general, difficult to decide whether a given set of generalized eigenvalues is the complete spectrum. As long as N is sufficiently small, one may hope that the spectra $\{\mu_n(N)\}_{n=0}^{\infty}$ and the linear spectrum $\{\mu_n(0)\}_{n=0}^{\infty}$ are in one-to-one correspondence and that eigenvalues with the same index n are continuously connected when N is changed from a finite value to zero.

Above we have used the values of the wave function and its derivatives at $x_e = 0$ on each bond, altogether $4B$ real parameters. The complexity of stating $4B$ equations for $4B$ parameters can be reduced building in continuity at the vertices from the start, e.g by choosing a spanning tree and then building up a continuous solution on the spanning tree first. Further complexity reduction can be achieved by considering the flux p_η as a parameter on each edge; flux conservation implies that it is sufficient to know the flux on some edges (indeed just on the edges we took out to get a spanning tree) to obtain the flux on other edges explicitly.

D. Stationary Scattering States for an Open Graph

Large parts of the discussion in the previous chapter can be extended to open graphs with a finite number of leads. We just need to discuss proper conditions for the wave function $\phi_\ell(x_\ell)$ on the leads $\ell \in \mathcal{L}$ as $x_\ell \to \infty$. It is instructive to first recall the situation for an open linear quantum graph where $g_e = 0$ for all edges $e \in \mathcal{E}$ [8, 9]. In this case, basically two types of solutions exist: In the physics literature they are usually referred to as bound states and scattering states. The former have a discrete spectrum of eigenvalues and are square-integrable, the latter have a continuous spectrum and have a bounded amplitude on the leads (implying that they are not square-integrable over the complete open graph).

1. Bound states

The bound state on a linear finite open graph have a discrete spectrum of allowed values for the chemical potential. The corresponding wave function is either decaying exponentially $\phi_l \propto e^{-\kappa x_l}$ with a negative chemical potential $\mu = -\kappa^2 < 0$ (i.e., at the bottom of the spectrum), or the wave function vanishes on all leads. In the latter case there is a known topological mechanism that makes it possible to construct wave functions with positive chemical potential $\mu > 0$ which are supported on finite closed subgraphs (topological bound states). The topological bound states in a linear quantum graph are not generic in the sense that they require rational ratios of bond lengths.

In the nonlinear setting any bound states at the bottom of the spectrum come in one-parameter families such that the chemical potential depends on the number of particles (L^2-norm) in complete analogy to the solutions in finite graphs.

The topological mechanism for bound states may also be generalized to the nonlinear case; however, the number of conditions one has to impose makes it clear that topological bound states remain as non-generic as they are for the linear case (note that the condition of rational ratios of bond lengths needs to be replaced with a non-linear generalization). A detailed understanding of topological bound states for open nonlinear graphs is an interesting topic in its on right but not in the focus of the present work which is either on closed graphs or the scattering states of open graphs.

2. Scattering states

Let us start again with a discussion of the scattering states for a linear open quantum graph. These exist for any $\mu = k^2 > 0$ (the continuous spectrum of a graph). The wave function on the leads may be written as

$$\phi_l(x_l) = a_l e^{-ikx_l} + b_l e^{ikx_l}, \tag{27}$$

where a_l is the incoming amplitude and b_l the outgoing amplitude along the lead $l \in \mathcal{L}$. Physically, one may think of the amplitudes a_l as being fixed in an experiment and the outgoing amplitudes b_l as the response of the system that is to be measured. Indeed, if one satisfies all matching conditions inside the graph the outgoing amplitudes are related to the incoming by a linear transformation

$$b_l = \sum_{l'=1}^{L} S(k)_{ll'} a_{l'}, \tag{28}$$

where $S(k)$ is known as the *scattering matrix*. Total flux conservation implies that $S(k)$ is unitary. Explicitly the scattering matrix of an open linear graph is given by

$$S = \sigma_{\mathcal{LL}} + \sigma_{\mathcal{LB}} \left(1 - e^{ik\ell}\sigma_{\mathcal{BB}}\right)^{-1} e^{ik\ell}\sigma_{\mathcal{LB}} \tag{29}$$

where $e^{ik\ell} = \mathrm{diag}(e^{ik\ell_1}, \ldots, e^{ik\ell_B}, e^{ik\ell_1}, \ldots, e^{ik\ell_B})$ and the matrices $\sigma_{\mathcal{XY}}$ are constructed from the vertex scattering matrices as follows. The diagonal $L \times L$ matrix $\sigma_{\mathcal{LL}}$ contains all direct backscattering amplitudes at the vertices adjacent to the corresponding lead. The $L \times 2B$ matrix $\sigma_{\mathcal{LB}}$ contains the scattering amplitudes for scattering from a directed bond to an (outgoing) lead as the corresponding entry in the matrix (matrix elements that are not consistent with the directed edge connectivity vanish). Analogously, the $2B \times L$ matrix σ_{BL} contains the scattering amplitudes for scattering from a lead (incoming) to a directed bond, and the $2B \times 2B$ matrix σ_{BB} contains the internal scattering from one directed bond to another at some vertex.

The scattering matrix has a very clear physical interpretation in terms of an experiment where incoming waves are fixed by the setting and reflected or transmitted waves are measured. However, the incoming wave and the reflected wave can only be characterized independently if the superposition principle holds on the leads.

For $\mu = k^2 > 0$ this can only be achieved by setting $g_l = 0$ on all leads $l \in \mathcal{L}$. With this assumption equation (27) still describes the wave function on the leads such that the coefficients a_l are the amplitudes of the incoming wave which we assume to be given by the experimenter (theoretically as boundary conditions) and the coefficients b_l describe the measured response. In general they are nonlinear functions,

$$b_l = b_l(a_1, \ldots, a_L), \tag{30}$$

of the incoming amplitudes. For sufficiently small incoming amplitudes $|a_l|^2 \to 0$ one expects that the leading term is given in terms of the scattering matrix of the corresponding linear graph (i.e. setting $g_e = 0$ everywhere on the

graph)

$$b_l(a_1,\ldots,a_L) = \sum_{l'=1}^{L} S_{ll'}(k)a_{l'} + O(|a_1|^2,\ldots,|a_L|^2) \ . \tag{31}$$

Transmission and reflection can be defined if we have a single non-vanishing incoming amplitude on the lead $l \in \mathcal{L}$. In that case we may define the reflection coefficient as

$$R_l(a_l) = \frac{|b_l(0,\ldots,0,a_l,0,\ldots)|^2}{|a_l|^2} \tag{32}$$

and the transmission coefficient from lead l to lead l' as

$$T_{l'l}(a_l) = \frac{|b_{l'}(0,\ldots,0,a_l,0,\ldots)|^2}{|a_l|^2}. \tag{33}$$

Evaluating the functions $b_{l'}$ and the resulting reflection and transmission coefficients is one of the central theoretical physical problems for an open nonlinear quantum graph. Implicitly they are given by the set of local solutions on the edges with the matching conditions on the vertices as described before.

Let us conclude this section with two remarks.

i. The assumption $g_l = 0$ on the leads is not a severe restriction for $\mu > 0$. Indeed, if we have a scattering solution for a nonlinear open quantum graph where $g_l \neq 0$ for some lead $l \in \mathcal{L}$ then we may choose some point $x_{l,0} \geq 0$ on this lead and replace the solution for $x_l > x_{l,0}$ with (27) such that $\phi_l(x_l)$ and $\phi_l'(x_l)$ are continuous at $x_l = x_{l,0}$, while the solution for $x_l < x_{l,0}$ and all other edges remains unchanged. While the reflection and transmission amplitudes defined in this way will depend explicitly on the choice of $x_{l,0}$ (both the phase and the absolute values), such a construction allows us to discuss scattering solutions in analogy to linear wave scattering solutions.

ii. While for linear open graphs the continuous spectrum is always $\mu \geq 0$ it is possible to have scattering solutions on nonlinear open graphs where $\mu < 0$ (if $g_l < 0$ on some leads). In that case we may not just set $g_l = 0$ on all leads without changing the scattering solution on the bonds unless we are ready to accept solutions that grow in absolute value without bound along the leads. However, if we introduce a constant negative potential $-V_0 < 0$ along the leads such that $\mu + V_0 = k^2 > 0$, we may set $g_l = 0$ in an analogous way and then discuss scattering solutions in analogy to the case $\mu > 0$.

III.   HAMILTONIAN FORMALISM AND CANONICAL PERTURBATION THEORY FOR THE NLSE

The framework presented in the previous section makes it possible to reduce the problem of finding solutions to the NLSE on graphs to a finite set of (generally nonlinear) algebraic equations for a finite set of variables. Already for relatively simple graphs the complexity of solving these equations will not allow for explicit analytical solutions. Compared to the corresponding problem of finding solutions to the linear Schrödinger equations on graphs also a numerical approach is faced with a considerably increased complexity. In the second paper [1] of this series we will apply the framework to find some solutions for a few basic closed and open graph structures. In the face of the rising complexity of the problem when the number of edges grows we introduce an approximation scheme that assumes small amplitudes and allows for long edges $\ell_b \gg 1/k$ with a positive chemical potential $\mu = k^2 > 0$. This approximation scheme is based on standard canonical perturbation theory for the auxiliary Hamiltonian dynamics as described in textbooks [47, 48]. We start with formally defining exact action-angle variables for the system. These depend formally on the nonlinear coupling strength g. For $g \to 0$ the action-angle variables reduce to the well-known action angle variables of a two-dimensional isotropic harmonic oscillator. The exact action-angle variables at finite g can then be expressed as a formal expansion in g using canonical perturbation theory. We derive explicitly to lowest order in the cubic case $\nu = 1$.

There are several advantages of the canonical perturbation theory over a direct expansion of the wave function in the NLSE. In such an approach one sets $\phi(x) = \phi^{(0)}(x) + \delta\phi(x)$ where $\phi^{(0)}(x)$ is a solution of the linear Schrödinger equation and $\delta\phi(x) = \sum_{n=1}^{\infty} g^n \phi^{(n)}(x)$ accounts for the perturbation. Then one solves the equations order by order. In the most naive variant it is well known from the standard textbook example [48] that unphysical resonance effects increase the amplitude of oscillations in $\delta\phi(x)$ effectively destroying the applicability of the whole approach at a finite distance. More sophisticated variants of this approach (e.g. by adding formal expansion of other parameters, e.g. setting

$\mu = \mu^{(0)} + \sum_{n=1}^{\infty} g^n \mu^{(n)})$ may improve this but will to lowest order always keep the form $\phi(x) \approx \phi^{(0)}(x) + g\phi^{(1)}(x)$ where $g\phi^{(1)}(x)$ is supposed to be a small perturbation of the leading term for arbitrary (large) x.

The main root of the unphysical (and mathematically unwanted) resonance effects lies in the fact that the wavenumber changes when the system is perturbed. The unperturbed wave function is periodic and obeys $\phi(x) = \phi(x + 2\pi/k)$. The perturbed solutions are quasi-periodic with two (generally incommensurate for finite g) wave numbers. Using action-angle variables is the natural way to decouple these two underlying periods. Moreover this approach shows that the perturbations lead to two different effects: They change the local shape of the wave function and they change the wave numbers. While tiny changes of the shape are locally confined, even the most tiny shifts in the wavenumber lead to changes of the corresponding phases that can add up over large distances such that the wave function can no longer be written in the form $\phi(x) \approx \phi^{(0)}(x) + g\phi^{(1)}(x)$ in any consistent way. Indeed while we derive canonical perturbation theory formally as an expansion in the nonlinear coupling strength g the approach opens a number of asymptotic regimes in the cubic NLSE that we discuss at the end of the section.

A. Hamiltonian Formalism and Action-Angle Variables

As we have described the auxiliary dynamics in the Lagrangian approach it is straight forward to perform the standard Legendre transform and the corresponding change of variables $(r, \eta, dr/dx, d\eta/dx) \mapsto (r, \eta, p_r, p_\eta)$ where $p_r = dr/dx$ is the conjugate momentum to the variable r and p_η defined in (11) is the angular momentum conjugate to η. The Hamilton function is just the energy (12) expressed in the canonical variables $H = \frac{1}{2}p_r^2 + V_{\text{eff}}(p_\eta, r)$. As this is an integrable system the Hamiltonian equations of motion are simplified by introducing action-angle variables. We assume a positive chemical potential $\mu > 0$ for the rest of this section. This ensures oscillatory solutions for sufficiently small r and p_r. This is the region where we want to define action-angle variables. In the attractive case $g < 0$ the approach is valid in the whole phase space.

In the present context one action variable is the angular momentum

$$I_\eta \equiv p_\eta \tag{34}$$

which can take any value in $\mathbb{R}$. The second action variable can be expressed as the integral

$$I_r(H, I_\eta) = \frac{1}{\pi} \int_{r_-(H, I_\eta)}^{r_+(H, I_\eta)} \sqrt{2(H - V_{\text{eff}}(I_\eta, r))} dr \tag{35}$$

which is expressed as a function of the angular momentum and energy. Here $r_+(H, I_\eta)$ and $r_-(H, I_\eta) < r_+(H, I_\eta)$ are the turning points defined as solutions of $V_{eff}(I_\eta, r_\pm) = H$. Note that (35) implies $I_r \geq 0$ and implicitly defines the energy as a function of the action variables $H = H(I_r, I_\eta)$. Moreover, by expressing $H = p_r^2/2 + V_{\text{eff}}(p_\eta, r)$ Eq. (35) also defines the radial action as a function of the original phase space coordinates, i.e. $I_r = I_r(p_r, p_\eta, r)$.

This allows us to define a generating function for a canonical transformation $(r, p_r, \eta, p_\eta) \mapsto (\alpha_r, I_r, \alpha_\eta, I_\eta)$. We can write the generating function that depends on the original (generalised position) variables r and η and the new action variable I_r and I_η

$$S(I_r, r, I_\eta, \eta) = I_\eta \eta + \int_{r_0}^{r} p_r(I_r, I_\eta, r') dr' + F(I_r, I_\eta), \tag{36}$$

where $p_r(I_r, I_\eta, r)$ is defined implicitly by (35) and expressing $H = H(p_r, I_\eta, r)$. The function $F(I_r, I_\eta)$ can be chosen arbitrarily as it only affects a shift of the angle variables. The lower boundary r_0 of the integral in (36) is an arbitrary constant (in principle one may incorporate the effect of $F(I_r, I_\eta)$ into the lower boundary by letting it depend on the actions). The transformation is generated by taking derivatives of (36)

$$p_r = \frac{\partial S}{\partial r} = p_r(I_r, I_\eta, r) \tag{37a}$$

$$p_\eta = \frac{\partial S}{\partial \eta} = I_\eta \tag{37b}$$

$$\alpha_r = \frac{\partial S}{\partial I_r} = \frac{\partial F(I_r, I_\eta)}{\partial I_r} + \int_{r_0}^{r} \frac{\partial p_r(I_r, I_\eta, r')}{\partial I_r} dr' \tag{37c}$$

$$\alpha_\eta = \frac{\partial S}{\partial I_\eta} = \eta + \frac{\partial F(I_r, I_\eta)}{\partial I_\eta} + \int_{r_0}^{r} \frac{\partial p_r(I_r, I_\eta, r')}{\partial I_\eta} dr' . \tag{37d}$$

Here the first equation gives back (35) and the second gives $p_\eta = I_\eta$, as required. The third and fourth equations define the two angle variables α_r and α_η.

The complexity of the transformation to action-angle variables is accompanied by a corresponding simplification of the equations of motion. By construction the two action variables are constants of motion and the angle variables change linearly in time

$$\alpha_r(t) = \alpha_r(0) + \kappa_r(I_r, I_\eta)t \qquad \text{and} \qquad \alpha_\eta(t) = \alpha_\eta(0) + \kappa_\eta(I_r, I_\eta)t \tag{38}$$

where

$$\kappa_r = \frac{\partial H}{\partial I_r} \qquad \text{and} \qquad \kappa_\eta = \frac{\partial H}{\partial I_\eta} \ . \tag{39}$$

These two angular frequencies (or wave numbers in the original context) may be given in a slightly more explicit way as

$$\kappa_r = \frac{1}{\frac{\partial I_r}{\partial H}} \qquad \text{and} \qquad \kappa_\eta = -\frac{\frac{\partial I_r}{\partial I_\eta}}{\frac{\partial I_r}{\partial H}} \tag{40}$$

in terms of the function $I_r(H, I_\eta)$ as defined in (35). For the cubic case $\nu = 1$ we give exact expressions for $\partial I_r / \partial H$ and $\partial I_r / \partial I_\eta$ in Appendix B.

While the Hamiltonian description in action-angle variables does not seem to simplify the full solution of the problem it is a reformulation that will allow us to perform a systematic expansion that, at least in low orders, offers closed analytic expressions.

Our strategy will be to find approximate solutions to the transformation $(r, p_r, \eta, I_\eta) \mapsto (\alpha_r, I_r, \alpha_\eta, I_\eta)$ by *formally* considering the nonlinear coupling constant g as a small parameter. For this we write the original Hamiltonian as

$$H(p_r, I_\eta, r) = H_0(p_r, I_\eta, r) - g\frac{r^{2\nu+2}}{2\nu + 2}. \tag{41}$$

where $H_0(p_r, I_\eta, r)$ is the Hamilton function of the linear problem. We start with transforming to action-angle variables of the linear case and then use canonical perturbation theory to treat the additional term $g\frac{r^{2\nu+2}}{2\nu+2}$. Such a perturbative treatment is valid as long as the harmonic term in the effective potential dominates the anharmonic perturbation, that is $k^2 \frac{r^2}{2} \gg g\frac{r^{2\nu+2}}{2\nu+2}$ or

$$g\frac{r^{2\nu}}{(\nu + 1)k^2} \ll 1 \ . \tag{42}$$

As $\nu > 0$ the perturbative expansion will only be valid for small amplitudes and break down as soon as amplitudes are of size $r^2 \sim (k^2/g)^{1/\nu}$.

B. The linear case

If $g = 0$ the transformation to action-angle coordinates can be performed explicitly. In order to distinguish the action-angle variable for $g = 0$ from the exact action-angle variable for $g \neq 0$, we use the variables $(\beta_r, J_r, \beta_\eta, J_\eta)$ for $g = 0$ and reserve $(\alpha_r, I_r, \alpha_\eta, I_\eta)$ for the exact action-angle variables in the general case. With $J_\eta = p_\eta$ one may perform the corresponding integral in (35) to obtain

$$J_r(H_0, J_\eta) = \frac{H_0}{2k} - \frac{|J_\eta|}{2} \qquad \Leftrightarrow \qquad H_0(J_r, J_\eta) = k\left(2J_r + |J_\eta|\right) \ . \tag{43}$$

In the following we always consider H_0 as a function of J_r and J_η. The generating function (36) for the transformation can be expressed explicitly as

$$S_0(J_r, J_\eta, r, \eta) = J_\eta\eta + \frac{H_0}{2k}\left[a\sqrt{1 - u^2} + \arcsin(u) - \sqrt{1 - a^2}\arcsin\left(\frac{a + u}{1 + au}\right)\right] \tag{44}$$

where

$$a = \sqrt{1 - \frac{J_\eta^2 k^2}{H_0^2}} = \frac{2\sqrt{J_r(J_r + |J_\eta|)}}{2J_r + |J_\eta|} \tag{45a}$$

$$u = \frac{\frac{k^2 r^2}{H_0(J_r, J_\eta)} - 1}{a} . \tag{45b}$$

The resulting angle variables are

$$\beta_r = \arcsin(u) \tag{46a}$$

$$\beta_\eta = \eta - \frac{s_\eta}{2} \arccos\left(1 - \frac{2J_r(1 - u^2)}{(2J_r + |J_\eta|)(1 + au)}\right) \tag{46b}$$

where $s_\eta = \mathrm{sgn}(J_\eta) = J_\eta/|J_\eta|$.

Hamilton's equations in the action-angle variables leave the action variables J_r and J_η constant, while the angles change linearly

$$\beta_r(x) = 2kx + \beta_r(0) \quad \text{and} \quad \beta_\eta(x) = s_\eta kx + \beta_\eta(0) . \tag{47}$$

The wave function $\phi(x) = r(x)e^{i\eta(x)}$ can be expressed via

$$r(x) = \sqrt{\frac{2J_r + |J_\eta|}{k}} (1 + a\sin(\beta_r(x))) \tag{48a}$$

$$\eta(x) = \beta_\eta(x) + \frac{s_\eta}{2} \arccos\left(1 - \frac{2J_r \cos^2(\beta_r(x))}{(2J_r + |J_\eta|)(1 + a\sin(\beta_r(x)))}\right) \tag{48b}$$

$$\phi(x) = \frac{1}{\sqrt{k}} \left(\sqrt{J_r + |J_\eta|}e^{i\beta_\eta(x)} + is_\eta\sqrt{J_r}e^{i\beta_\eta(x) - is_\eta\beta_r(x)}\right) \tag{48c}$$

in terms of action-angle variables. Using $s_\eta = \pm 1$ and the solutions (47) (with vanishing initial angles) the exponentials in (48c) reduce to the well known solutions $e^{i\beta_\eta(x)} = e^{\pm ikx}$ and $e^{i\beta_\eta(x) - is_\eta\beta_r(x)} = e^{\mp is_\eta kx}$. Note also that (48a) implies

$$\frac{\left(\sqrt{J_r + |J_\eta|} - \sqrt{J_r}\right)^2}{k} \leq r(x)^2 \leq \frac{\left(\sqrt{J_r + |J_\eta|} + \sqrt{J_r}\right)^2}{k} \tag{49}$$

and $r(x)^2 = |\phi(x)|^2$ oscillates betweens these bounds with a wavelength π/k.

While (48c) seems a complicated way to write a quite trivial solution it is the starting point of the canonical perturbation theory that will take into account the nonlinearity. In the regime of weak nonlinearity, i.e. $gr^{2\nu} \ll k^2$ we will see that the accumulated effect of the nonlinearity over large distances can be captured to leading order by keeping the form of the wave function (48c) and replacing k in (47) with two perturbed wave numbers $\kappa_r(J_r, J_\eta)$ and $\kappa_\eta(J_r, J_\eta)$ which will depend on the action variables.

C. Canonical perturbation theory

After having found action-angle variables $(\beta_r, J_r, \beta_\eta, J_\eta)$ for the linear case let us now write the full nonlinear Hamilton function in terms of these action-angle variable

$$H(J_r, J_\eta, \beta_r) = H_0(J_r, J_\eta) + gG_0(J_r, J_\eta, \beta_r) \tag{50}$$

where

$$G_0(J_r, J_\eta, \beta_r) = -\frac{\left(2J_r + |J_\eta| + 2\sqrt{J_r(J_r + |J_\eta|)}\sin(\beta_r)\right)^{\nu+1}}{k^{\nu+1}(2\nu + 2)} \tag{51}$$

The perturbative parameter which is considered small in the following is $gr^{2\nu}/k^2 \ll 1$ (see (42)). Using (49) this is equivalent to requiring

$$\frac{g(J_r + |J_\eta|)^\nu}{k^{2+\nu}} \ll 1 \tag{52}$$

or $g \ll k^{2+\nu}/(J_r + |J_\eta|)^\nu$.

In n-th order perturbation theory we want to find transformed action-angle variables $(\alpha_r^{(n)}, I_r^{(n)}, \alpha_\eta^{(n)}, I_\eta^{(n)})$ such that the Hamilton function expressed in new variables becomes

$$H = H_0(J_r, J_\eta) + gG_0(J_r, J_\eta, \beta_r) \equiv H_n(I_r^{(n)}, I_\eta^{(n)}) + g^{n+1}G_{n+1}(I_r^{(n)}, I_\eta^{(n)}, \beta_r) \tag{53}$$

where $\beta_r = \beta_r(I_r^{(n)}, I_\eta^{(n)}, \alpha_r^{(n)})$. For $n = 0$ we set $I_r^{(0)} = J_r$, $I_\eta^{(0)} = J_\eta$, $\alpha_r^{(0)} = \beta_r$ and $\alpha_\eta^{(0)} = \beta_\eta$. To find the generating function of the canonical transformation, one uses the ansatz

$$S_n(I_r^{(n)}, I_\eta^{(n)}, \beta_r, \beta_\eta) = I_r^{(n)}\beta_r + I_\eta^{(n)}\beta_\eta + \sum_{m=1}^{n} g^m F_m(I_r^{(n)}, I_\eta^{(n)}, \beta_r) \tag{54}$$

where the functions $F_m(I_r^{(n)}, I_\eta^{(n)}, \beta_r)$ are periodic in β_r and found by the requirement that the generated transformation

$$J_r = \frac{\partial S_n}{\partial \beta_r} = I_r^{(n)} + \sum_{m=1}^{n} g^m \frac{\partial F_m}{\partial \beta_r} \tag{55a}$$

$$J_\eta = \frac{\partial S}{\partial \beta_\eta} = I_\eta^{(n)} \tag{55b}$$

$$\alpha_r^{(n)} = \frac{\partial S}{\partial I_r^{(n)}} = \beta_r + \sum_{m=1}^{n} g^m \frac{\partial F_m}{\partial I_r^{(n)}} \tag{55c}$$

$$\alpha_\eta^{(n)} = \frac{\partial S}{\partial I_\eta^{(n)}} = \beta_\eta + \sum_{m=1}^{n} g^m \frac{\partial F_m}{\partial I_\eta^{(n)}} \tag{55d}$$

leads to the cancellation of all terms involving β_r up to n-th order in (53). This can be done in an iterative manner by expanding $H_0(I_r^{(n)} + \sum_{m=1}^{n} g^m \frac{\partial F_m}{\partial \beta_r}, I_\eta^{(n)})$ and $G_0(I_r^{(n)} + \sum_{m=1}^{n} g^m \frac{\partial F_m}{\partial \beta_r}, I_\eta^{(n)}, \beta_r)$ in orders of g and demanding that the terms cancel order by order. If all F_m for $m \le n$ are found, one can immediately proceed to the order $n+1$ in the perturbation theory where the known functions F_m may be kept and only F_{n+1} needs to be found.

In first order perturbation theory one finds

$$H_0 + gG_0 = k\left(2I_r^{(1)} + |I_\eta|^{(1)}\right) + 2gk\frac{\partial F_1}{\partial \beta_r} - \frac{g}{k^{\nu+1}(2\nu+2)}\left(2I_r^{(1)} + |I_\eta^{(1)}| + 2\sqrt{I_r^{(1)}(I_r^{(1)} + |I_\eta^{(1)}|)}\sin(\beta_r)\right)^{\nu+1} + O(g^2) . \tag{56}$$

This can be solved in principle for any $\nu > 0$ by writing $F_1(I_r^{(1)}, I_\eta^{(1)}, \beta_r) = \sum_{N=-\infty}^{\infty} f_{1N}(I_r^{(1)}, I_\eta^{(1)})e^{i\beta_r N}$ and requiring that $ikN f_{1N}(I_r^{(1)}, I_\eta^{(1)})$ cancels the corresponding Fourier coefficient of gG_0.

Let us here focus on the most relevant case of the cubic nonlinearity ($\nu = 1$), where (56) reduces to

$$H_0 + gG_0 = k\left(2I_r^{(1)} + |I_\eta|^{(1)}\right) - \frac{g}{4k^2}\left(6I_r^{(1)^2} + 6I_r^{(1)}|I_\eta^{(1)}| + I_\eta^{(1)^2}\right)$$
$$+ 2gk\frac{\partial F_1}{\partial \beta_r} - \frac{g}{2k^2}\left(2(2I_r^{(1)} + |I_\eta^{(1)}|)\sqrt{I_r^{(1)}(I_r^{(1)} + |I_\eta^{(1)}|)}\sin(\beta_r) - I_r^{(1)}(I_r^{(1)} + |I_\eta^{(1)}|)\cos(2\beta_r)\right) + O(g^2) \tag{57}$$

where the term in the second line cancels by choosing

$$F_1 = -\frac{1}{2k^3}(2I_r^{(1)} + |I_\eta^{(1)}|)\sqrt{I_r^{(1)}(I_r^{(1)} + |I_\eta^{(1)}|)}\cos(\beta_r) - \frac{1}{8k^3}I_r^{(1)}(I_r^{(1)} + |I_\eta^{(1)}|)\sin(2\beta_r) . \tag{58}$$

and the Hamilton function is $H = H_1(I_r^{(1)}, I_\eta^{(1)}) + g^2 G_1(I_r^{(1)}, I_\eta^{(1)}, \beta_r)$ with

$$H_1(I_r^{(1)}, I_\eta^{(1)}) = k\left(2I_r^{(1)} + |I_\eta^{(1)}|\right) - \frac{g}{4k^2}\left(6I_r^{(1)^2} + 6I_r^{(1)}|I_\eta^{(1)}| + I_\eta^{(1)^2}\right) . \tag{59}$$

Neglecting quadratic orders in g, the original action-angle variables can be expressed in terms of the new ones as

$$J_r = I_r^{(1)} + \frac{g}{4k^3}\left(2(2I_r^{(1)} + |I_\eta^{(1)}|)\sqrt{I_r^{(1)}(I_r^{(1)} + |I_\eta^{(1)}|)}\sin(\alpha_r^{(1)}) - I_r^{(1)}(I_r^{(1)} + |I_\eta^{(1)}|)\cos(2\alpha_r^{(1)})\right) \tag{60a}$$

$$J_\eta = I_\eta^{(1)} \tag{60b}$$

$$\beta_r = \alpha_r^{(1)} + \frac{g}{8k^3}\left(\frac{16I_r^{(1)2} + 16I_r^{(1)}|I_\eta^{(1)}| + 2I_\eta^{(1)2}}{\sqrt{I_r^{(1)}(I_r^{(1)} + |I_\eta^{(1)}|)}}\cos(\alpha_r^{(1)}) + (2I_r^{(1)} + |I_\eta^{(1)}|)\sin(2\alpha_r^{(1)})\right) \tag{60c}$$

$$\beta_\eta = \alpha_\eta^{(1)} + s_\eta\frac{g}{8k^3}\left(\frac{8I_r^{(1)2} + 6I_r^{(1)}|I_\eta^{(1)}|}{\sqrt{I_r^{(1)}(I_r^{(1)} + |I_\eta^{(1)}|)}}\cos(\alpha_r^{(1)}) + I_r^{(1)}\sin(2\alpha_r^{(1)})\right) \tag{60d}$$

where $s_\eta = \mathrm{sgn}(I_\eta^{(1)})$.

The solution of the Hamiltonian dynamics in first order perturbation theory leaves the action variables $I_r^{(1)}$ and $I_\eta^{(1)}$ constant, while the conjugate angles increase as

$$\alpha_r^{(1)}(x) = \kappa_r^{(1)}(I_r^{(1)}, I_\eta^{(1)})x + \alpha_r^{(1)}(0) \tag{61a}$$

$$\alpha_\eta^{(1)}(x) = \kappa_\eta^{(1)}(I_r^{(1)}, I_\eta^{(1)})x + \alpha_\eta^{(1)}(0) \tag{61b}$$

where

$$\kappa_r^{(1)}(I_r^{(1)}, I_\eta^{(1)}) = \frac{\partial H_1}{\partial I_r^{(1)}} = 2k\left(1 - \frac{3g}{4k^3}(2I_r^{(1)} + |I_\eta^{(1)}|)\right) \tag{62a}$$

$$\kappa_\eta^{(1)}(I_r^{(1)}, I_\eta^{(1)}) = \frac{\partial H_1}{\partial I_\eta^{(1)}} = s_\eta k\left(1 - \frac{g}{2k^3}(3I_r^{(1)} + |I_\eta^{(1)}|)\right)\ . \tag{62b}$$

Substitution of this solution into (48c) gives an approximate local solution for the stationary NLSE to first order in $\frac{g(I_r^{(1)} + |I_\eta^{(1)}|)}{k^3} \ll 1$.

D. The asymptotic regimes of the nonlinear transfer operator in canonical perturbation theory

In order to understand the significance of the approximate solutions to the NLSE in canonical perturbation theory to lowest nontrivial order, let us consider the nonlinear transfer operator along some edge of length ℓ in the graph. For this purpose it is not necessary to consider the full nonlinear transfer operator in its most general form. It will be sufficient to restrict the 'initial' conditions at $x = 0$ to $\phi(0) = 0$ (while the derivative takes some real value) and only consider the wave function at the other end of the edge. In first-order canonical perturbation theory, this is given by

$$\phi(\ell) = 2\sqrt{\frac{J_r(\ell)}{k}}\sin\left(\frac{\beta_r(x)}{2}\right), \tag{63a}$$

$$J_r(\ell) = I_r - \frac{gI_r^2}{4k^3}(4\cos(\alpha_r(\ell)) - \cos(2\alpha_r(\ell))) + O\left(\frac{g^2I_r^3}{k^6}\right), \tag{63b}$$

$$\beta_r(\ell) = \alpha_r(\ell) + \frac{gI_r}{4k^3}(8\sin(\alpha_r(\ell)) - \sin(2\alpha_r(\ell))) + O\left(\frac{g^2I_r^2}{k^6}\right), \tag{63c}$$

$$\alpha_r(\ell) = \kappa_r\ell, \tag{63d}$$

$$\kappa_r = 2k\left(1 - \frac{3gI_r}{2k^3} + O\left(\frac{g^2I^2}{k^6}\right)\right)\ . \tag{63e}$$

This is a real solution where only one action-angle pair is relevant. While this special case does not show the dephasing between the two degrees of freedom that are present for more general initial conditions, the explicitly given error estimates will be sufficient to identify the relevant asymptotic regimes and these regimes remain unaltered in the general case. Equations (63) are justified for locally weak nonlinearity which really means that the dimensionless strength of nonlinearity is negligible $\frac{|g||\phi|^2}{k^2} \propto \frac{gI_r}{k^3} \ll 1$. Equations (63) also reveal two entirely different effects of a

weak nonlinearity on a solution. The first effect is a local deformation of the linear solution. The second effect is a phase shift due to the nonlinear wave numbers κ_r. Our approach assumed locally weak nonlinearity which implies that the local deformations (which are of relative order $\frac{|g|\overline{I_r}}{k^3}$) are always small. However the accumulated change in the phase (which is of order $\frac{|g|\overline{I_r}\ell}{k^2}$) does not necessarily need to be small.

One may identify three different asymptotic regimes that are consistent with the canonical perturbation expansion. Each may lead to additional consistent simplifications.

R1 The *low-intensity weakly nonlinear asymptotic regime* $g\overline{|\phi|^2} \to 0$ at fixed (bounded) wavenumber k. This is equivalent to either $g \to 0$ or $I_r \to 0$ (and $I_\eta \to 0$ for general initial conditions) when all other parameters are fixed. This regime is weak in both the local and the global sense. For the leading nonlinear effects one may expand the oscillatory functions with respect to the small phase shifts (where this leads to a simplification).

R2 The *short wavelength globally weak nonlinear asymptotic regime* $k \to \infty$ with $g\overline{|\phi_e|^2}$ fixed (bounded). This is similar to the low-intensity regime in that it is weakly nonlinear in both the local and the global sense. It leads to additional simplifications as the dominant nonlinear effects all come from the shift in the nonlinear wave number κ_r (and κ_η for general initial conditions).

R3 The *short wavelength asymptotic regime with moderately large intensities* $k \to \infty$ and $\frac{g\overline{|\phi|^2}}{k^2} \to 0$. This regime is weakly nonlinear only in the local but not (necessarily) in the global sense and the intensity is allowed to have moderately large values. As in the globally weak short wavelength regime the leading effect is the shift of the nonlinear wave number κ_r (and κ_η) which leads to phase shifts of order $\frac{g\ell\overline{|\phi|^2}}{k}$. As these phase shifts may be large we may *not* expand the oscillatory terms and the nonlinear effect in the wavefunction comes in the leading order. If we are only interested in the leading effect we may neglect all other deformations altogether. In this regime the equations that describe the stationary states on nonlinear quantum graphs simplify considerably in form but remain nonlinear.

The explicit leading order of the wavenumber shift is consistent as long as the intensity is only growing moderately as $\overline{|\phi|^2} = O(k)$ (at fixed g and ℓ). The regime, however, allows a larger growth $\overline{|\phi_e|^2} = o(k^2)$ but this requires to calculate the nonlinear wavenumber κ_r (and κ_η for general initial conditions) to all orders which is done in Appendix B.

In [1] we will consider a number of simple graph structures as case studies how these regimes can be explored with our approach. To come back to the discussion we had at the beginning of this section, let us compare again our approach to any perturbation theory based on writing the wave function in the form $\phi(x) = \phi_0(x) + \delta\phi(x)$ where $\phi_0(x)$ is a solution of the corresponding linear equation and $\delta\phi(x)$ a small perturbation. In the asymptotic regimes R1 and R2 consistency requires that equations (63) are expanded further with respect to small parameters which leads to the form $\phi(x) = \phi_0(x) + \delta\phi(x)$. So our approach contains standard perturbation theory as a special case. As regimes R1 and R2 can be obtained by linearization of the of the NLSE with respect to $\delta\phi(x)$ no genuine nonlinear effects such as bifurcations or multistability can be described. Regime R3 however is not consistent with a small perturbation of the wavefunction and cannot be obtained by linearization of the NLSE in standard perturbation theory. We will show that genuine nonlinear effects can be described in this regime for sufficiently simple graph structures in [1].

If necessary it is not conceptually difficult to obtain higher order approximations in the canonical perturbation theory though the expressions become more and more cumbersome; using symbolic computer algebra software is the obvious choice.

IV. CONCLUSION

In this paper we considered the stationary NLSE on open and closed metric graphs, in short nonlinear quantum graphs, as a model that makes it possible to investigate topological effects on nonlinear waves. The solutions consist of stationary solutions of the one-dimensional NLSE on the edges (finite intervals or half lines) that obey matching conditions at the edges. We have given a complete qualitative description of all local solutions, including solutions that may form singularities when extended beyond the interval that represents a finite edge (bond). Our qualitative analysis uses an exact equivalence between the NLSE in one dimension and the dynamics of a particle in two dimensions and a central potential where the spatial variable x takes the role of the time. The chemical potential (or energy) μ, nonlinear coupling constant g, and the power of the nonlinearity ν characterize both the NLSE and the corresponding central potential in the equivalent dynamics. The Hamiltonian energy and the angular momentum are two constants of motion for the equivalent dynamical system. They characterise the trajectories and hence the local solutions of the NLSE. Scaling properties make it possible to reduce the analysis to $\mu = \pm 1$ and $g = \pm 1$. For $\nu = 1$ we compile

the complete set of analytic solutions in the Appendix; so far these have been given explicitly only for solutions that remain bounded on an infinite interval.

The knowledge of the solutions along each edge formally reduces the problem of characterising the solutions on a graph to a finite set of nonlinear equations that follow from the matching conditions and a nonlinear transfer operator that expresses the wave function and its derivative at one end of an edge in terms of the values at the other end. While these equations may be solved numerically complete analytical solutions will generally be hard to find even for quite simple graphs. In order to simplify the nonlinear transfer operator we have introduced a canonical perturbation theory for the NLSE valid for small g (and arbitrary ν). This is a very powerful tool. In contrast to diagrammatic approaches which only yield corrections linear in g for quantities such as the wave function, in the canonical perturbation theory g enters the wave function in a nonlinear way.

We have here focused on the NLSE on quantum graphs. Generalizations to other nonlinear wave equation can be worked out in an analogous way. Such generalizations may be necessary for physical applications of the framework. For example, the NLSE appears in nonlinear optics in a specific approximation where the envelope of an optical field is considered. Backscattering from the vertices implies that this approximation may break down and more general wave equations (not necessarily for a scalar wave) need to be considered. For the qualitative understanding of the combined effect of nonlinear wave propagation and network topology the nonlinear quantum graphs based on the simpler NLSE is rich in complexity and may give already a lot of insight.

In the second paper of this series [1] we will analyze some basic closed and open graph structures analytically and numerically. Among other things we will show that using the canonical perturbation theory described here allows for an analytical description of genuine non-linear effects. We will also give an outlook on open questions.

Appendix A: Analytic Local Solutions on a Given Edge for $\nu = 1$ in Terms of Jacobi Elliptic Functions

The bounded stationary solutions for the cubic NLSE ($\nu = 1$) on the infinite line or a ring are known and can be expressed in terms of elliptic functions [49, 50]. The construction of stationary solutions on graphs requires the knowledge of *all* local solutions including those that are unbounded when continued to the infinite line. These can also be reduced to elliptic functions. As we are not aware that these have been discussed in the literature we here give a complete overview of all local solutions of the one-dimensional cubic stationary NLSE. Due to the scaling laws (18) and (19) it is sufficient to consider solutions

$$\phi(x) = R_{\pm 1, \pm 1}(x; r_0, p_\eta, H, \sigma)e^{i\vartheta_{\pm 1, \pm 1}(x; r_0, p_\eta, H, \sigma)}$$

for chemical potential $\mu = \pm 1$ and nonlinear coupling $g = \pm 1$. We also state expressions for the integrated intensity (scaled number of particles)

$$N_{\pm 1, \pm 1}(x; r_0, p_\eta, H, \sigma) := \int_0^x |\phi(x')|^2 dx' = \int_0^x R_{\pm 1, \pm 1}(x'; r_0, p_\eta, H, \sigma)^2 dx' \tag{A1}$$

over an interval $[0, x]$.

1. Elliptic integrals and elliptic functions

We use the following definitions for elliptic integrals (the Jacobi form)

$$F(x|m) := \int_0^x \frac{1}{\sqrt{1 - u^2}\sqrt{1 - m\,u^2}} du \tag{A2a}$$

$$K(m) := F(1|m) \tag{A2b}$$

$$E(x|m) := \int_0^x \frac{\sqrt{1 - m\,u^2}}{\sqrt{1 - u^2}} du \tag{A2c}$$

$$\Pi(x|a, m) := \int_0^x \frac{1}{\sqrt{1 - u^2}\sqrt{1 - m\,u^2}(1 - a\,u^2)} du \tag{A2d}$$

where $0 \leq x \leq 1$, $m \leq 1$ and $a \leq 1$. Note that our definition allows m and a to be negative.
The notation in the literature is far from uniform. Our choice seems the most concise for the present context and it is usually straight forward to translate our definitions into the ones of any standard reference on special functions. For instance, the *NIST Handbook of Mathematical Functions* [49] defines the three elliptical integrals $F(\phi, k)$, $E(\phi, k)$

and $\Pi(\phi, \alpha, k)$ by setting $x = \sin(\phi)$, $m = k^2$, and $a = \alpha^2$ in our definitions above.

Jacobi's Elliptic function $\text{sn}(x, m)$, the elliptic sine, is defined as the inverse of $F(u|m)$

$$u = \text{sn}(x, m) \qquad \Leftrightarrow \qquad x = F(u|m) . \tag{A3}$$

This defines $\text{sn}(x, m)$ for $x \in [0, K(m)]$. This is extended to a periodic function with period $4K(m)$ by requiring $\text{sn}(K(m) + x, m) = \text{sn}(K(m) - x, m)$, $\text{sn}(-x, m) = -\text{sn}(x, m)$ and $\text{sn}(x + 4K(m), m) = \text{sn}(x, m)$. So, $\text{sn}(x, m)$ is an elliptic generalization of $\sin(x)$. The corresponding elliptic cosine $\text{cn}(x, m)$ is obtained by requiring that it is a continuous function satisfying

$$\text{cn}^2(x, m) + \text{sn}^2(x, m) = 1 \tag{A4}$$

such that $\text{cn}(0, m) = 1$. It is useful to also define the non-negative function

$$\text{dn}(x, m) := \sqrt{1 - m \, \text{sn}^2(x, m)}. \tag{A5}$$

At $m = 0$ and $m = 1$ the elliptic functions can be expressed as

$$\text{sn}(x, 0) = \sin x, \qquad\qquad \text{sn}(x, 1) = \tanh x, \tag{A6a}$$
$$\text{cn}(x, 0) = \cos x, \qquad\qquad \text{cn}(x, 1) = \cosh^{-1} x, \tag{A6b}$$
$$\text{dn}(x, 0) = 1, \qquad\qquad \text{dn}(x, 1) = \cosh^{-1} x . \tag{A6c}$$

Derivatives of elliptic functions can be expressed in terms of elliptic functions

$$\frac{d}{dx}\text{sn}(x, m) = \text{cn}(x, m)\text{dn}(x, m), \tag{A7a}$$

$$\frac{d}{dx}\text{cn}(x, m) = -\text{sn}(x, m)\text{dn}(x, m), \tag{A7b}$$

$$\frac{d}{dx}\text{dn}(x, m) = -m \, \text{sn}(x, m)\text{cn}(x, m) . \tag{A7c}$$

The first of these equations implies that $u = \text{sn}(x, m)$ is a solution of the first order ordinary differential equation

$$\frac{du}{dx} = \sqrt{1 - u^2}\sqrt{1 - mu^2} . \tag{A8}$$

2. Repulsive case with positive chemical potential

In the main text we have used the constants of motion p_η and H as parameters for the formal solutions for arbitrary nonlinear exponent ν. For $\nu = 1$ a different (equivalent) set of real parameters that we denote by ρ_i ($i = 1, 2, 3$) are more useful. For the repulsive case with positive chemical potential ($g = 1$ and $\mu = 1$) they are implicitly defined (given arbitrary real values for p_η and H) by

$$\rho_1 + \rho_2 + \rho_3 = 2 \tag{A9a}$$
$$\frac{1}{\rho_1} + \frac{1}{\rho_2} + \frac{1}{\rho_3} = \frac{2H}{p_\eta^2} \tag{A9b}$$
$$\rho_1 \rho_2 \rho_3 = 2p_\eta^2 \tag{A9c}$$

or, equivalently, through the identity

$$P(R) := (R^2 - \rho_1)(R^2 - \rho_2)(R^2 - \rho_3) = R^6 - 2R^4 + 4HR^2 - 2p_\eta^2 \tag{A10}$$

of real polynomials in R^2. Note that the sign of p_η does not enter the definition of the parameters ρ_i. The differential equation for the amplitude $R_{1,1}(x)$ then reduces to $2R^2 \left(\frac{dR}{dx}\right)^2 = P(R)$ where the left-hand side is non-negative. This implies that the solutions will have amplitudes in the intervals where $P(R) > 0$.

Note that (A10) defines $P(R)$ as a real polynomial of order three in R^2. We thus expect that either all three ρ_i are real, or two ρ_i are complex and one is real.

In the first case with three real ρ_i we may order them as $0 \leq \rho_1 \leq \rho_2 \leq \rho_3 \leq 2$ where the first and last inequalities

follow straight forwardly from Eq. (A9). The motion is either bounded with $\rho_1 \leq R_{1,1}(x)^2 \leq \rho_2$ or unbounded with $R_{1,1}(x)^2 > \rho_3$. If $\rho_2 = \rho_3$ then three solutions coexist: a bounded dark soliton with $\rho_1 \leq R_{1,1}(x)^2 \leq \rho_2$, a constant amplitude solutions $R_{1,1}(x)^2 = \rho_2 \equiv \rho_3$ and an unbounded solution with $R_{1,1}(x)^2 \geq \rho_2 \equiv \rho_3$.

In the complex case we may choose ρ_3 real and write $\rho_1 = \xi + i\chi$ and $\rho_2 = \xi - i\chi$. The motion is unbounded with $R_{1,1}(x)^2 > \rho_3$. Note, that in either case $r_0 \equiv R_{1,1}(0)$ has to be chosen consistently with the inequalities valid for $R_{1,1}(x)$.

a. Bounded solutions: $\rho_1 \leq R_{1,1}(x)^2 \leq \rho_2 \leq \rho_3$

With the initial conditions $R(0) = r_0$ and $\vartheta(0) = 0$ the bounded solution with real ρ_i is given by

$$R_{1,1}(x) = \sqrt{\rho_1 + (\rho_2 - \rho_1)\, u(x)^2} \tag{A11a}$$

$$\vartheta_{1,1}(x) = \frac{p_\eta}{\sigma \beta \rho_1} \left[2n\Pi\left(1|-a, m\right) + (-1)^n \Pi\left(u(x)|-a, m\right) - \Pi(u_0|-a, m) \right] \tag{A11b}$$

$$N_{1,1}(x) = \rho_3 x - \frac{\rho_3 - \rho_1}{\sigma \beta} \left[2nE(1|m) + (-1)^n E(u(x)|m) - E(u_0|m) \right] \tag{A11c}$$

$$u(x) = \mathrm{sn}\left(y_0 + \sigma \beta x, m\right) \tag{A11d}$$

where $m = \frac{\rho_2 - \rho_1}{\rho_3 - \rho_1}$, $a = \frac{\rho_2 - \rho_1}{\rho_1}$, $\beta = \sqrt{\frac{\rho_3 - \rho_1}{2}}$, $u_0 = \sqrt{\frac{r_0^2 - \rho_1}{\rho_2 - \rho_1}}$, $y_0 = F\left(u_0|m\right)$ and $n \in \mathbb{Z}$ such that $\left| \frac{y_0 + \sigma \beta x}{K(m)} - 2n \right| \leq 1$.

The first line (A11a) is the substitution that reduces the ordinary differential equation $2R^2 \left(\frac{dR}{dx}\right)^2 = P(R)$ for $R_{1,1}(x)$ to (A8) for $u(x)$.

For $\rho_2 = \rho_1$ this reduces to a constant amplitude solution

$$R_{1,1}(x; r_0, p_\eta, H, \sigma) = \sqrt{\rho_1} \tag{A12a}$$

$$\vartheta_{1,1}(x; r_0, p_\eta, H, \sigma) = \frac{p_\eta}{\rho_1} x \tag{A12b}$$

$$N_{1,1}(x; r_0, p_\eta, H, \sigma) = \rho_1 x \ . \tag{A12c}$$

b. Unbounded solutions: $\rho_1 \leq \rho_2 \leq \rho_3 \leq R_{1,1}(x)^2$

The unbounded solution for real ρ_i is given by

$$R_{1,1}(x; r_0, p_\eta, H, \sigma) = \sqrt{\rho_2 + (\rho_3 - \rho_2) \frac{1}{1 - u(x)^2}} \tag{A13a}$$

$$\vartheta_{1,1}(x; r_0, p_\eta, H, \sigma) = \frac{p_\eta}{\rho_2} x - \frac{p_\eta(\rho_3 - \rho_2)}{\sigma \beta \rho_2 \rho_3} \left[2n\Pi\left(1|a, m\right) + (-1)^n \Pi\left(u(x)|a, m\right) - \Pi(u_0|a, m) \right] \tag{A13b}$$

$$N_{1,1}(x; r_0, p_\eta, H, \sigma) = \begin{cases} \rho_3 x - \frac{\rho_3 - \rho_1}{\sigma \beta} \left[E\left(u(x)|m\right) - E(u_0|m) \right] + \\ \quad \frac{\rho_3 - \rho_1}{\sigma \beta} \left[u(x)\sqrt{\frac{1 - m u(x)^2}{1 - u(x)^2}} - u_0 \sqrt{\frac{1 - m u_0^2}{1 - u_0^2}} \right] & \text{if } n = 0; \\[2mm] \infty & \text{if } n \neq 0. \end{cases} \tag{A13c}$$

$$u(x) = \mathrm{sn}\left(y_0 + \sigma \beta x, m\right) \tag{A13d}$$

where $m = \frac{\rho_2 - \rho_1}{\rho_3 - \rho_1}$, $a = \frac{\rho_2}{\rho_3}$, $\beta = \sqrt{\frac{\rho_3 - \rho_1}{2}}$, $u_0 = \sqrt{\frac{r_0^2 - \rho_3}{r_0^2 - \rho_2}}$, $y_0 = F\left(u_0|m\right)$ and $n \in \mathbb{Z}$ such that $\left| \frac{y_0 + \sigma \beta x}{K(m)} - 2n \right| \leq 1$.

<center>*c. Special case: $\rho_1 < \rho_2 = \rho_3$*</center>

Three solutions coexist: a bounded dark soliton solution, a constant amplitude solution, and an unbounded solution. The dark soliton can be obtained from setting $\rho_2 = \rho_3$ in (A11) which then reduces to

$$R_{1,1}(x; r_0, p_\eta, H, \sigma) = \sqrt{\rho_1 + (\rho_2 - \rho_1)\, u(x)^2} \tag{A14a}$$

$$\vartheta_{1,1}(x; r_0, p_\eta, H, \sigma) = \frac{p_\eta}{\rho_2}x + \frac{p_\eta \sqrt{2}}{\sigma \rho_2 \sqrt{\rho_1}}\left[\arctan\left(\sqrt{a}\,u(x)\right) - \arctan\left(\sqrt{a}\,u_0\right)\right] \tag{A14b}$$

$$N_{1,1}(x; r_0, p_\eta, H, \sigma) = \rho_2 x - \frac{\rho_2 - \rho_1}{\sigma\beta}\left[u(x) - u_0\right] \tag{A14c}$$

$$u(x) = \tanh\left(y_0 + \sigma\beta x\right) \tag{A14d}$$

where $a = \frac{\rho_2 - \rho_1}{\rho_1}$, $\beta = \sqrt{\frac{\rho_2 - \rho_1}{2}}$, $u_0 = \sqrt{\frac{r_0^2 - \rho_1}{\rho_2 - \rho_1}}$ and $y_0 = \operatorname{arctanh}(u_0)$. The constant amplitude solution is given by

$$R_{1,1}(x; r_0, p_\eta, H, \sigma) = \sqrt{\rho_2} \tag{A15a}$$

$$\vartheta_{1,1}(x; r_0, p_\eta, H, \sigma) = \frac{p_\eta}{\rho_2}x \tag{A15b}$$

$$N_{1,1}(x; r_0, p_\eta, H, \sigma) = \rho_2 x \ , \tag{A15c}$$

and the unbounded solution is

$$R_{1,1}(x; r_0, p_\eta, H, \sigma) = \sqrt{\rho_1 + (\rho_2 - \rho_1)\, u(x)^{-2}} \tag{A16a}$$

$$\vartheta_{1,1}(x; r_0, p_\eta, H, \sigma) = \frac{p_\eta}{\rho_2}x + \frac{p_\eta \sqrt{2}}{\sigma \rho_2 \sqrt{\rho_1}}\left[\arctan\left(\frac{u(x)}{\sqrt{a}}\right) - \arctan\left(\frac{u_0}{\sqrt{a}}\right)\right] \tag{A16b}$$

$$N_{1,1}(x; r_0, p_\eta, H, \sigma) = \begin{cases} \rho_2 x + \frac{\rho_2 - \rho_1}{\sigma\beta}\left[\frac{1}{u(x)} - \frac{1}{u_0}\right] & \text{if } y_0 - \beta\sigma x > 0; \\ \infty & \text{if } y_0 - \beta\sigma x \leq 0 \end{cases} \tag{A16c}$$

$$u(x) = \tanh\left(y_0 - \sigma\beta x\right) \tag{A16d}$$

where $\beta = \sqrt{\frac{\rho_2 - \rho_1}{2}}$, $u_0 = \sqrt{\frac{r_0^2 - \rho_1}{\rho_2 - \rho_1}}$ and $y_0 = \operatorname{arctanh}(u_0)$. Equations (A15) and (A16) can be obtained from (A13) by performing appropriate limits $\rho_2 \to \rho_3$.

<center>*d. Unbounded solutions: $R_{1,1}(x)^2 \geq \rho_3 > 1$, $\rho_1 = \xi + i\chi = \rho_2^*$*</center>

This is given by

$$R_{1,1}(x; r_0, p_\eta, H, \sigma) = \sqrt{\rho_3 + \gamma\frac{u(x)^2(1 - m\, u(x)^2)}{1 - u(x)^2}} \tag{A17a}$$

$$\vartheta_{1,1}(x; r_0, p_\eta, H, \sigma) = \frac{p_\eta}{\rho_3 \beta \sigma (a - b)}\Big[(1 - b)\left[2n\Pi(1|b, m) + (-1)^n \Pi\left(u(x)|b, m\right) - \Pi(u_0|b, m)\right] -$$

$$(1 - a)\left[2n\Pi(1|a, m) + (-1)^n \Pi\left(u(x)|a, m\right) - \Pi(u_0|a, m)\right]\Big] \tag{A17b}$$

$$N_{1,1}(x; r_0, p_\eta, H, \sigma) = \begin{cases} (\rho_3 + \gamma)x - \frac{2\gamma}{\sigma\beta}\left[E\left(u(x)|m\right) - E(u_0|m)\right] + \\ \quad \frac{\gamma}{\sigma\beta}\left[u(x)\sqrt{\frac{1 - m\, u(x)^2}{1 - u(x)^2}} - u_0\sqrt{\frac{1 - m\, u_0^2}{1 - u_0^2}}\right] & \text{if } n = 0 \\ \\ \infty & \text{if } n \neq 0 \end{cases} \tag{A17c}$$

$$u(x) = \operatorname{sn}\left(y_0 + \sigma\beta x, m\right) \tag{A17d}$$

where $\gamma = \sqrt{(\rho_3 - \xi)^2 + \chi^2}$, $m = \frac{\gamma - \rho_3 + \xi}{2\gamma}$, $\beta = \sqrt{\gamma/2}$, $u_0 = \sqrt{\frac{\gamma + r_0^2 - \rho_3}{\gamma - \rho_3 + \xi} + \sqrt{\left(\frac{\gamma + r_0^2 - \rho_3}{\gamma - \rho_3 + \xi}\right)^2 - \frac{2(r_0^2 - \rho_3)}{\gamma - \rho_3 + \xi}}}$, $y_0 = F\left(u_0|m\right)$, $a = \frac{\rho_3 - \gamma + \sqrt{\xi^2 + \chi^2}}{2\rho_3}$, $b = \frac{\rho_3 - \gamma - \sqrt{\xi^2 + \chi^2}}{2\rho_3}$, and $n \in \mathbb{Z}$ such that $\left|\frac{y_0 + \sigma\beta x}{K(m)} - 2n\right| \leq 1$.

3. Repulsive case with negative chemical potential

For the solutions with $g = 1$ and $\mu = -1$ the three parameters ρ_i $(i = 1, 2, 3)$ are defined by

$$\rho_1 + \rho_2 + \rho_3 = -2 \tag{A18a}$$

$$\frac{1}{\rho_1} + \frac{1}{\rho_2} + \frac{1}{\rho_3} = \frac{2H}{p_\eta^2} \tag{A18b}$$

$$\rho_1 \rho_2 \rho_3 = 2p_\eta^2 \tag{A18c}$$

or, equivalently

$$P(R) = (R^2 - \rho_1)(R^2 - \rho_2)(R^2 - \rho_3) = R^6 + 2R^4 + 4HR^2 - 2p_\eta^2 \ . \tag{A19}$$

As in the previous case either all three ρ_i are real, or two ρ_i are complex and one is real.
In the first case with three real ρ_i we may order them as $\rho_1 \leq \rho_2 \leq 0 \leq \rho_3 \leq 2$ where the second and third inequalities can be shown straight forwardly. In the complex case we may choose ρ_3 real and write $\rho_1 = \xi + i\chi$ and $\rho_2 = \xi - i\chi$. In both cases the motion is unbounded with $R_{1,-1}(x)^2 > \rho_3$.

a. Unbounded solutions: $\rho_1 \leq \rho_2 \leq 0 \leq \rho_3 \leq R_{1,-1}(x)^2$

These solutions obey the same formulas as the unbounded motion (A13) – note however, that the parameters ρ_i have different restrictions. Analogously, the special case $\rho_2 = \rho_3 = 0$ can be obtained from (A16).

b. Unbounded solutions: $R_{1,-1}(x)^2 \geq \rho_3 > 1$, $\rho_1 = \xi + i\chi = \rho_2^*$

These solutions obey the same formulas as the unbounded motion (A17).

4. Attractive case with positive chemical potential

For the solutions with $g = -1$ and $\mu = 1$ the three parameters ρ_i $(i = 1, 2, 3)$ are defined by

$$\rho_1 + \rho_2 + \rho_3 = -2 \tag{A20a}$$

$$\frac{1}{\rho_1} + \frac{1}{\rho_2} + \frac{1}{\rho_3} = \frac{2H}{p_\eta^2} > 0 \tag{A20b}$$

$$\rho_1 \rho_2 \rho_3 = -2p_\eta^2 \tag{A20c}$$

or, equivalently,

$$P(R) = (\rho_1 - R^2)(\rho_2 - R^2)(\rho_3 - R^2) = -R^6 - 2R^4 + 4HR^2 - 2p_\eta^2 \ . \tag{A21}$$

The right-hand side defines $P(R)$ as real polynomial in R^2, so either all ρ_i are real, or one is real and two are complex conjugates. The latter case can however be excluded. Indeed the differential equation for the amplitude $R_{-1,1}(x)$ is of the form $2R^2 \left(\frac{dR}{dx}\right)^2 = P(R) \geq 0$ which requires $P(R)$ to be positive. However, if $\rho_3 = \rho_2^*$, then $\rho_1 < 0$ (because $\rho_1 \rho_2 \rho_3 = \rho_1 |\rho_2|^2 = -2p_\eta^2 < 0$) and $P(R) = (\rho_1 - R^2)|\rho_2 - R^2|^2 < 0$ for all real values of R.
We are left with the case that all ρ_i are real and we may order them as $\rho_1 \leq 0 \leq \rho_2 \leq \rho_3$, where the first and second inequalities can be shown straight forwardly. The solution is bounded with $\rho_2 \leq R_{-1,1}(x)^2 \leq \rho_3$ and given by

$$R_{-1,1}(x; r_0, p_\eta, H, \sigma) = \sqrt{\rho_3 - (\rho_3 - \rho_2)\frac{1 - u(x)^2}{1 - m\,u(x)^2}} = \sqrt{\rho_1 + (\rho_2 - \rho_1)\frac{1}{1 - m\,u(x)^2}} \tag{A22a}$$

$$\vartheta_{-1,1}(x; r_0, p_\eta, H, \sigma) = \frac{p_\eta}{\rho_1}x + \frac{p_\eta(\rho_1 - \rho_2)}{\sigma\beta\rho_1\rho_2}\left[2n\Pi(1|a, m) + (-1)^n\Pi\left(u(x)|a, m\right) - \Pi(u_0|a, m)\right] \tag{A22b}$$

$$N_{-1,1}(x; r_0, p_\eta, H, \sigma) = \rho_1 x + \frac{\rho_2 - \rho_1}{\sigma\beta}\left[2n\Pi(1|m, m) + (-1)^n\Pi\left(u(x)|m, m\right) - \Pi(u_0|m, m)\right] \tag{A22c}$$

$$u(x) = \operatorname{sn}\left(y_0 + \sigma\beta x, m\right) \tag{A22d}$$

where $m = \frac{\rho_3 - \rho_2}{\rho_3 - \rho_1}$, $a = \frac{\rho_1}{\rho_2}m$, $\beta = \sqrt{\frac{\rho_3 - \rho_1}{2}}$, $u_0 = \sqrt{\frac{1}{m}\frac{r_0^2 - \rho_2}{r_0^2 - \rho_1}}$, $y_0 = F\left(u_0|m\right)$ and $n \in \mathbb{Z}$ such that $\left|\frac{y_0 + \sigma\beta x}{K(m)} - 2n\right| \leq 1$.

5. Attractive case with negative chemical potential

For the solutions with $g = -1$ and $\mu = -1$ the three parameters ρ_i $(i = 1, 2, 3)$ are defined by

$$\rho_1 + \rho_2 + \rho_3 = 2 \tag{A23a}$$

$$\frac{1}{\rho_1} + \frac{1}{\rho_2} + \frac{1}{\rho_3} = \frac{2H}{p_\eta^2} \tag{A23b}$$

$$\rho_1 \rho_2 \rho_3 = -2p_\eta^2 \tag{A23c}$$

or, equivalently

$$P(R) = (\rho_1 - R^2)(\rho_2 - R^2)(\rho_3 - R^2) = -R^6 + 2R^4 + 4HR^2 - 2p_\eta^2 . \tag{A24}$$

Analogously to the previous case all ρ_i have to be real with $\rho_1 \leq 0 \leq \rho_2 \leq \rho_3 \leq 2$. The solution is bounded with $\rho_2 \leq R_{-1,-1}(x)^2 \leq \rho_3$ and the formulas (A22) remain valid.
The special case of the soliton $\rho_2 = \rho_1 = 0$ $(p_\eta = 0$ and $H = 0)$ deserves some attention as the expression (A22) formally vanishes. The limit $\rho_2, \rho_1 \to 0$ at fixed r_0 is however not trivial. This solution is given explicitly by

$$R_{-1,-1}(x; r_0, p_\eta, H, \sigma) = \frac{\sqrt{2}}{\cosh(y_0 - \sigma x)} \tag{A25a}$$

$$\vartheta_{-1,-1}(x; r_0, p_\eta, H, \sigma) = 0 \tag{A25b}$$

$$N_{-1,-1}(x; r_0, p_\eta, H, \sigma) = \frac{2}{\sigma}(\tanh(y_0) - \tanh(y_0 - \sigma x)) \tag{A25c}$$

where $y_0 = \operatorname{arccosh}\left(\sqrt{2}/r_0\right)$.

Appendix B: Exact expressions for the angular frequencies for the cubic NLSE

The two angular frequencies κ_r and κ_η in Eq. (40) follow from $\partial I_r/\partial H$ and $\partial I_r/\partial I_\eta$ with $I_r(H, I_\eta)$ defined in Eq. (35). In the cubic case $\nu = 1$ they are given explicitly by

$$\frac{\partial I_r}{\partial H} = \frac{1}{\pi} \int_{r_-}^{r_+} \frac{dr}{\sqrt{\left(4Hr^2 - 2I_\eta^2 \mp 2r^4 \pm r^6\right)/(2r^2)}} \tag{B1}$$

and

$$\frac{\partial I_r}{\partial I_\eta} = -\frac{I_\eta}{\pi} \int_{r_-}^{r_+} \frac{dr}{r^2\sqrt{\left(4Hr^2 - 2I_\eta^2 \mp 2r^4 \pm r^6\right)/(2r^2)}} \tag{B2}$$

with r_- and r_+ the two turning points of the dynamics that obey the condition $r_- < r_+$. We calculate them here explicitly for $\mu = \pm 1$ and $g = \pm 1$. We include here the unbounded solutions where $r_+ \equiv \infty$.

1. Repulsive case with positive chemical potential

a. Bounded solutions: $\rho_1 \leq R_{1,1}(x)^2 \leq \rho_2 \leq \rho_3$

Here the r-variable in Eqs. (B1) and (B2) is restricted to values between $\sqrt{\rho_1}$ and $\sqrt{\rho_2}$. Using the parametrization in Eq. (A10) we can express the integral in (B1) as

$$\frac{\partial I_r}{\partial H} = \frac{1}{\pi} \int_{\sqrt{\rho_1}}^{\sqrt{\rho_2}} \frac{dr}{\sqrt{(r^2 - \rho_1)(r^2 - \rho_2)(r^2 - \rho_3)/(2r^2)}} \tag{B3}$$

and the one in (B2) as

$$\frac{\partial I_r}{\partial I_\eta} = -\frac{I_\eta}{\pi} \int_{\sqrt{\rho_1}}^{\sqrt{\rho_2}} \frac{dr}{r^2\sqrt{(r^2 - \rho_1)(r^2 - \rho_2)(r^2 - \rho_3)/(2r^2)}}. \tag{B4}$$

The final result is

$$\frac{\partial I_r}{\partial H} = \frac{1}{\pi\beta} K(m) \tag{B5}$$

and

$$\frac{\partial I_r}{\partial I_\eta} = -\frac{I_\eta}{\pi\beta\rho_1} \Pi\left(1|a,m\right) \tag{B6}$$

with the functions $K(m)$ and $\Pi\left(1|a,m\right)$ defined in Eq. (A2), m, β and a are defined in terms of ρ_1, ρ_2 and ρ_3 after Eq. (A11).

b. Unbounded solutions $\rho_1 \leq \rho_2 \leq \rho_3 \leq R_{1,1}(x)^2$

In this case the r-dynamics is restricted by the condition $r \geq \sqrt{\rho_3}$, we obtain

$$\frac{\partial I_r}{\partial H} = \frac{1}{\pi\beta} K(m) \tag{B7}$$

and

$$\frac{\partial I_r}{\partial I_\eta} = -\frac{I_\eta}{\pi} \left[\frac{1}{\rho_2\beta} K(m) - \frac{\rho_3 - \rho_2}{\rho_2\rho_3\beta} \Pi\left(1|a,m\right)\right] \tag{B8}$$

with m, β and a as defined after Eq. (A13).

c. Special case: $\rho_1 < \rho_2 = \rho = 3$

Due to the singularity resulting from the term proportional to $\left(r^2 - \rho_2\right)^{-1}$ the considered quantities tend to infinity in this case.

d. Unbounded solutions: $R_{1,1} \geq \rho_3 > 1$, $\rho_1 = \xi + i\chi = \rho_2^*$

Here the motion takes place in the region $r \geq \sqrt{\rho_3}$, the quantities of interest are given by

$$\frac{\partial I_r}{\partial H} = \frac{1}{\pi\beta} K(m) \tag{B9}$$

and

$$\frac{\partial I_r}{\partial I_\eta} = -\frac{I_\eta}{\pi\beta(a-b)} \left[(1-b)\Pi(1|b,m) - (1-a)\Pi(1|a,m)\right] \tag{B10}$$

with m, β, a and b defined after Eq. (A17).

2. Repulsive case with negative chemical potential

Here unbounded motion is obtained, Eqs. (B3) and (B4) remain valid and the results from (B 1 b) and (B 1 d) remain applicable.

3. Attractive case with positive chemical potential

Here Eqs. (B3) and (B4) are changed to

$$\frac{\partial I_r}{\partial H} = \frac{1}{\pi} \int_{\sqrt{\rho_2}}^{\sqrt{\rho_3}} \frac{dr}{\sqrt{(\rho_1 - r^2)(\rho_2 - r^2)(\rho_3 - r^2)/(2r^2)}} \tag{B11}$$

and

$$\frac{\partial I_r}{\partial I_\eta} = -\frac{I_\eta}{\pi} \int_{\sqrt{\rho_2}}^{\sqrt{\rho_3}} \frac{dr}{r^2 \sqrt{(\rho_1 - r^2)(\rho_2 - r^2)(\rho_3 - r^2)/(2r^2)}} \tag{B12}$$

and finally result in

$$\frac{\partial I_r}{\partial H} = \frac{1}{\pi\beta} K(m) \tag{B13}$$

and

$$\frac{\partial I_r}{\partial I_\eta} = -\frac{I_\eta}{\rho_1\beta\pi} K(m) - \frac{I_\eta(\rho_1 - \rho_2)}{\beta\rho_1\rho_2\pi} \Pi(1|a, m) \tag{B14}$$

with β, m and a defined after Eq. (A22).

4. Attractive case with negative chemical potential

In this case the expressions from the last section remain valid, in the special case $\rho_2 = \rho_1 = 0$, $\partial I_r/\partial H$ and $\partial I_r/\partial I_\eta$ diverge due to the singularity of the r-integral at zero.

ACKNOWLEDGMENTS

[1] S. Gnutzmann, D. Waltner, *in preparation*
[2] T. Kottos, U. Smilansky, Ann. Phys. **274**, 76 (1999);
[3] S. Gnutzmann, U. Smilansky, Adv. Phys. **55**, 527 (2006).
[4] G. Berkolaiko, P. Kuchment, Introduction to Quantum Graphs, Mathematical Surveys and Monographs 186 (Providence, RI: American Mathematical Society, 2013).
[5] T. Kottos, U. Smilansky, Phys. Rev. Lett. **79**, 4794 (1997).
[6] S. Gnutzmann, A. Altland, Phys. Rev. Lett. **93**, 194101 (2004).
[7] S. Gnutzmann, J.P. Keating, F. Piotet, Ann. Phys. **325**, 2595 (2010).
[8] T. Kottos, U. Smilansky, Phys. Rev. Lett. **85**, 968 (2000);
[9] T. Kottos, U. Smilansky, J. Phys. A **36** 3501 (2003).
[10] Z. Pluhař, H.A. Weidenmüller. Phys. Rev. Lett. **110**, 034101 (2013).
[11] J. M. Zhang, F. C. Cui, D. L. Zhou, W. M. Liu, Phys. Rev. A **79**, 033401 (2009).
[12] T. Paul, K. Richter, P. Schlagheck, Phys. Rev. Lett. **94**, 020404 (2005).
[13] M. Hartung, T. Wellens, C. A. Müller, K. Richter, P. Schlagheck, Phys. Rev. Lett. **101**, 020603 (2008).
[14] K. Rapedius, D. Witthaut, H. J. Korsch, Phys. Rev. A **73**, 033608 (2006); K. Rapedius, H. J. Korsch, Phys. Rev. A **77**, 063610 (2008).
[15] P. Leboeuf, N. Pavloff, Phys. Rev. A **64**, 033602 (2001).
[16] S. Gnutzmann, U. Smilansky, S. Derevyanko, Phys. Rev. A **83**, 033831 (2011).
[17] S. Gnutzmann, H. Schanz, U. Smilansky, Phys. Rev. Lett. **110**, 094101 (2013).
[18] R. Lytel, S. Shafei, J.H. Smith, M.G. Kuzyk, Phys. Rev. A **87**, 043824 (2013).
[19] R. Adami, C. Cacciapuoti, D. Finco, D. Noja, Europhys. Lett. **100**, 10003 (2012).

[20] R. Adami, D. Noja, Commun. Math. Phys. **318**, 247 (2013).
[21] R. Adami, C. Cacciapuoti, D. Finco, D. Noja, J. Diff. Eq. **257**, 247 (2014).
[22] R. Adami, C. Cacciapuoti, D. Finco, D. Noja, J. Phys. A: Math. Theor. **45**, 192001 (2012).
[23] R. Adami, C. Cacciapuoti, D. Finco, D. Noja, Ann. I. H. Poincare **31**, 1289 (2014).
[24] C. Cacciapuoti, D. Finco, D. Noja, Phys. Rev. E **91**, 013206 (2015).
[25] D. Noja, D. Pelinovsky, G. Shaikhova, Nonlinearity **28**, 2343 (2015)
[26] R. Adami, C. Cacciapuoti, D. Finco, D. Noja, Rev. Math. Phys. **23**, 409 (2011).
[27] Z. Sobirov, D. Matrasulov, K. Sabirov, S. Sawada, K. Nakamura, Phys. Rev. E **81**, 066602 (2010).
[28] J. Holmer, J. Marzuola, M. Zworski, Commun. Math. Phys. **274**, 187 (2007).
[29] H. Uecker, D. Grieser, Z. Sobirov, D. Babajanov, D. Matrasulov, Phys. Rev. E **91**, 023209 (2015).
[30] V. Caudrelier, Commun. Math. Phys. **338**, 893 (2015).
[31] A. Tokuno, M. Oshikawa, and E. Demler, Phys. Rev. Lett. **100**, 140402 (2008).
[32] N. V. Hung, M. Trippenbach, B. A. Malomed, Phys. Rev. A **84**, 053618 (2011).
[33] A. E. Miroshnichenko, M. I. Molina, Y. S. Kivshar, Phys. Rev. E **75**, 046602 (2007).
[34] R. Burioni, D. Cassi, P. Sodano, A. Trombettoni, A. Vezzani, Physica D **216**, 71 (2006).
[35] M. Stojanovic, A. Maluckov, L. J. Hadzievski, B. A. Malomed, Physica D **240**, 14489 (2011).
[36] Y. Linzon, R. Morandotti, M. Volatier, V. Aimez, R. Ares, S. Bar-Ad, Phys. Rev. Lett. **99**, 133901 (2007).
[37] M. Peccianti, A. Dyadyusha, M. Kaczmarek, G. Assanto, Phys. Rev. Lett. **101**, 153902 (2008).
[38] D. Noja, Phil. Trans. R. Soc. A **372**, 20130002 (2013).
[39] L. D. Carr, C. W. Clark, W. P. Reinhardt, Phys. Rev. A **62**, 063610 (2000);
[40] L. D. Carr, C. W. Clark, W. P. Reinhardt, Phys. Rev. A **62**, 063611 (2000).
[41] Any choice of a coordinate system as described above implicitly implies a choice of direction on each edge – however we treat all coordinate systems that attribute the same distance to any two points as equivalent. For, example, on each bond we may switch from the initial coordinates to the equivalent coordinates $\hat{x}_b = \ell_b - x_b$ which traverse the bond in the opposite direction.
[42] L. Bergé, Phys. Rep. **303**, 259 (1998).
[43] V. Kostrykin, R. Schrader, J. Phys. A **32**, 595 (1999).
[44] Vertices of valency two with standard matching conditions and the same value of the nonlinear coupling constant g on either side can effectively be deleted by joining the two adjacent edges to one single edge of combined length.
[45] V. E. Zakharov, A. B. Shabat, Soviet Phys. JETP **34**, 62 (1972); russian original ZhETF **61**, 118 (1971).
[46] M. J. Ablowitz, *Nonlinear dispersive waves. Asymptotic analysis and solitons*, Cambridge University Press (2011).
[47] A. J. Lichtenberg, M. A. Lieberman, *Canonical Perturbation Theory*, Springer (1992).
[48] M. Tabor, *Chaos and Integrability in Nonlinear Dynamics*, Wiley (1989).
[49] F.W.J. Olver, D.W. Lozier, R.F. Boisvert, C.W. Clark, *NIST Handbook of Mathematical Functions* (Cambridge University Press, 2010).
[50] I. S. Gradstheyn, I. M. Ryzhik, *Table of Integrals, Series and Products*, Academic Press (1980).